

1 **Editor Decision: Publish subject to revisions (further review by Editor and Referees) (20**
2 **Oct 2016) by Miriam Coenders-Gerrits**

3 **Comments to the Author:**

4 The authors present a study where they test an ANN to upscale instantaneous remote sensing
5 observations (Rsi, RsiTOA, RSdTOA, theta_z, and L_D) to daily Rsd estimates from where
6 they estimate daily ET. These results are also compared to two other methods for converting
7 instantaneous observations to daily ET estimates. The paper is well written and easy to read.
8 Two reviewers were mainly positive, and the 3rd reviewer expressed some concerns on the
9 validity/usefulness of the method during (partly) overcast days. I think the authors correctly
10 replied to comments of the 3 reviewers and the proposed changes are OK. However, all 3
11 reviewers commented on the selection of the FLUXNET sites. How representative are the
12 sites for different climates, biomes and time of the year/seasonality?? Although the authors
13 replied to Reviewer #1 that they will elaborate on it, but that they already showed that it does
14 not influence the training of the ANN, I think the study will benefit from a proof of this claim.
15 Especially, since the main objective of the paper is to show the use of ANN for upscaling
16 from instantaneous to daily. Therefore, I agree with the suggestion of Reviewer #1 to do a
17 'sensitivity' analysis for the selection of the sites in place, time and biome.

18 **Response:** A sensitivity analysis is now performed to assess the applicability of the ANN-
19 based modeling framework to multiple biomes. The results are discussed in section 3.5.
20

21 **Minor comments:**

22 (1) P3L2 and L12: what is the need of using E_T and ETd? Are they not the same?

23 **Response:** By *ET*, we mean evapotranspiration, which is generic. *ET_d* signifies daily *ET* and
24 *ET_i* signifies instantaneous *ET*. This uniformity is maintained throughout the manuscript.

25 (2) P3L3: all symbols in text in italic (throughout manuscript)

26 **Response:** Done as suggested.

27 (3) P4L11: "... variables (e.g., dialy..." (add comma).

1 **Response:** This sentence is modified as follows (p4, l15 to l19):

2 Although the EF_r -based method produced comparable ET_d estimates as the R_s -based method,
3 however the dependence of EF_r estimates on certain variables (e.g., daily net available
4 energy; ϕ and wind speed) and the difficulty to characterise them at the daily scale from single
5 acquisition of polar orbiting satellites (Tang et al., 2015) makes it a relatively less attractive
6 method.

7 (4) P4L11: theta is not explained.

8 **Response:** It is net available energy, explained now (p4, l17).

9 (5) P5L2: better: "... predict Rsd based on Rsi satellite observations"

10 **Response:** Corrected (p5,l31).

11 (6) P5L2-4: Objectives 2 and 3 are not really objectives of this paper (since this is already
12 done in the past). It's more that the results of the ANN are used to apply one method to
13 upscale instantaneous observations to ETd and that these outcomes are then compared to two
14 other upscaling techniques.

15 **Response:** Objective is now moved to the end of the introduction (p5 l30 – l31; p6 11 – 13).

16 Objectives are corrected as follows,

17 The objectives of the present study are: (1) using a ANN with Multilayer Perceptron (MLP)
18 architecture to predict R_{Sd} based on R_{Si} satellite observations, (2) applying R_{Sd}/R_{Si} ratio as a
19 scaling factor to upscale ET_i to ET_d under all sky conditions, and (3) comparing the
20 performance of proposed R_s -based ET_i upscaling method with R_sTOA and EF -based ET_i
21 upscaling methods across a range of temporal scales, biomes and variable sky conditions.

22 (7) P6L7-10: What is the use of having ET with the units MJ/m²/d and Rsd in W/m²? Please
23 use one of the two for both.

24 **Response:** Necessary corrections are done (p6, l10 – l14).

25 (8) P7L12: add space between (Rye et al, 2012) and mainly.

- 1 **Response: Corrected (p8, l21).**
- 2 (9) P7L18: What is PURELIN? Please briefly explain.
- 3 **Response: Explained now (p8, l28 – l31).**
- 4 (10) P8L23-25: I would link here to figure 1 and use the same letters for the 3 method. Thus
5 a=Rs-method, b= RsdTOA-method and c=EF-method.
- 6 **Response: Necessary corrections are made (section 2.4, p10, l7 – l17).**
- 7 (11) Eq5: combine into 1 equation, Eq6: combine into 1 equation
- 8 **Response: Now all the equations are numbered individually (section 2.4 and 2.5, p10, p11).**
- 9 (12) P9L13-16: Use here the same order as the order of Eq8-12
- 10 **Response: Corrected now (section 2.5, p11, l9 – l11).**
- 11 (13) P10L10: Unclear/vague sentence. Please rewrite.
- 12 **Response: Corrected now (p12, l17 – l18).**
- 13 (14) P10L13: suggestion: use time-of-day instead of time-of-daytime.
- 14 **Response: Corrected throughout in the text.**
- 15 (15) P11L2: The categories of Tau are not explained in the text. When is something belonging
16 to Tau_1 and when to Tau_4? (like explained in the caption of fig 5.)
- 17 **Response: The categories of Tau is already explained in section 2.4 (p11, l2 – l5). For clarity,
18 we again explain it (p12, l29).**
- 19 (16) Table 2: Maybe make it more clear that "Rs, RsdTOA and EF" are the 3 methods and not
20 that e.g., the R2 refers to the performance of an estimation of Rs.
- 21 **Response: This is now made explicit in the caption of Table 2.**
- 22 (17) Table 1, 2,3: Maybe convert these tables into similar graphs like figure 11.

1 Response: We would prefer to keep Table 1, 2, 3 as they are in the manuscript. Representing
2 all of them in figures similar to Fig. 11 might add monotony.

3 Fig 1: What is the difference between Rsd_pred and Rsd?

4 Response: RSd_pred is the predicted RSd from RSi. Here RSd is the generic symbol to
5 signify daily shortwave radiation. We made the necessary correction in caption of Figure 1
6 caption.

7 Fig 5-caption: "...between Rsd_obs versus Rsd_pred...". Furthermore, also explain the
8 transmissivity classes in the main manuscript text.

9 Response: Corrected accordingly.

10 Fig 10: this figure is hard to read. Improve quality.

11 Response Corrected now.

12

13

14

15

16

17

18

19

20

21

22

1 **Reviewer 1 (R1):**

2 **1. Energy budget closure problem at FLUXNET.** Energy budget imbalance has long been
3 identified at FLUXNET sites. The imbalance is about -40% - +20%, indicating latent
4 heat/sensible heat fluxes might be underestimated by up to 40%. Indeed, the energy
5 imbalance is an existing fact we have to accept, I guess there is little can be done to
6 overcome it in this particular study.

7 **Response:** Good point. We have now included an intercomparison of R_s -based ET_i
8 upscaling results including both energy balance closure and non-closure in the revised
9 version of the manuscript ([p20 \[section 3.4\], Table 4](#)).

10 **2.** But my concerning is: if an ANN model is trained by FLUXNET data, how much
11 confidence do we have when we apply it to satellite retrieval? The energy budget close
12 problem affects the results in two ways: (1) the overall robustness of the proposed
13 upscaling method (R_s method); (2) comparison of R_s method with the evaporative
14 fraction based upscaling (EF method Eqn. 5). However, the exo-atmospheric irradiance
15 method is not affected (Eqn. 6). I guess the authors must be aware of this issue; it would
16 be better to literally discuss them in the results section.

17 **Response:** Regarding R1's concern on the impact of surface energy balance closure on
18 the performance of ET_d evaluation, **it is important to mention that the implicit
19 assumption in remote sensing based ET_i retrieval is the closure of surface energy
20 balance.** Therefore, for the remote sensing retrievals, the energy balance closure problems
21 will not affect ET_d estimates in the current framework of ANN. **However, for the
22 validation of remote sensing based ET_d retrievals, surface energy balance fluxes from
23 eddy covariance measurements need to be closed. This is now mentioned in section
24 3.4 ([p20 \[section 3.4\]](#))**

25 In the present study, the closure problem of surface energy balance will affect the
26 evaluation statistics of all the three methods, and therefore, we included an
27 intercomparison of R_s -based ET_i upscaling results including both energy balance closure
28 and non-closure in the revised version ([Table 4, section 3.4](#)). **As compared to the EF and
29 R_s TOA approach, the R_s -based method is more robust with regards to ET scaling on**

1 **a daily time frame since the method carries maximum information on the cloudiness,**
2 **which is a key limiting factor in upscaling of ET_i to ET_d .**

3 With reference to Eq. (1), the network developed is intended to develop an operational
4 method to directly upscale ET_i (estimated from polar orbiting satellites) to ET_d based on
5 the ratio of daily to instantaneous shortwave radiation (R_{Sd} and R_{Si}). Given there is no
6 direct method to directly estimate R_{Sd} from remote sensing satellite, we trained an ANN
7 with the FLUXNET observations of R_{Si} and R_{Sd} , and validated the model to predict R_{Sd}
8 over independent sites, followed by using R_{Sd}/R_{Si} ratio to convert ET_i to ET_d . The datasets
9 used for the ANN development covers a wide range of biome, climate, and variable sky
10 conditions. Therefore, we assume the R_{Sd} prediction from ANN to capture a broad
11 spectrum of radiative forcing, which is also reflected in the independent validation of R_{Sd}
12 and ET_d (Fig. 5, Fig. 7, Table 2). The performance of this model for satellite retrieval of
13 R_{Sd} (from R_{Si}) is dependent on the accuracy of R_{Si} retrieval (Loew, Peng, & Borsche,
14 2016). We have discussed these in the conclusion section (p21, 110 – 126). Also, the
15 distribution of sites over the tropics, Africa, and SE Asia are poor, and more sites over
16 these regions are expected to make the ANN model more robust, which is mentioned in
17 the revised manuscript (p21, 124 – 126).

18 Regarding R1's concern on the robustness of the approach, we have performed a
19 sensitivity analysis of R_s -based ANN performance by training ANN with data from
20 different biome combinations and compared ET_d prediction statistics of the different
21 combinations (section 3.5, Figure 13).

22 3. **Cloudy-sky issue.** The biggest problem of the proposed upscaling method (Rs method) is
23 that the ANN model does not include any information about “cloudiness”. Therefore,
24 model performance under cloudy-sky condition (or low atmospheric transmissivity) is
25 much worse than clear-sky condition. One way to tackle it, is to use climatology
26 precipitation data. Rainfall (highly related to cloudiness) has seasonal pattern, at least for
27 some regions (e.g., tropical rainforest, savanna). Similarly, dry season-wet seasons could
28 provide ANN model with additional information about “possibility” of the “cloudy-sky
29 condition” during a certain time period. In Figure 7, the overestimation of ET under
30 cloudy sky condition is “systematic”, meaning there might be a simple way to

1 “systematically” down regulate the ET as long as the ANN model knows it’s a cloudy
2 day.

3 **Response:** Good suggestion indeed. Following R1’s suggestion, we tested this hypothesis
4 by including the precipitation and soil moisture information with R_S and trained a new
5 ANN to evaluate if the inclusion of precipitation and soil moisture improved the
6 performance of ET_d prediction under persistent cloudy-sky conditions. This shows
7 substantial improvement in ET_d prediction under cloudy-sky cases [[section 3.2 \(p15, 11 – 127\) \(Figure 9\)](#)].

9 Including cloudiness as an input variable of the network during training process would
10 significantly enhance the performance of the network. Use of daily precipitation and soil
11 moisture as an indicator of cloudiness would have been the most appropriate approach in
12 this circumstance. However the cloud information available from alternative sources e.g.
13 from the Clouds and Earth’s Radiant Energy System (CERES), the International Satellite
14 Cloud Climatology Project–Flux Data (ISCCP-FD), and Global Energy and Water cycle
15 Experiment Surface Radiation Budget (GEWEX-SRB) are available at coarse spatial
16 resolution and there will be a scale mismatch. However, the precipitation data was not
17 consistently available for most of the sites and the data gaps were significant to alter the
18 sampling sizes. However for future studies, including cloudiness or daily precipitation as a
19 variable in the training of the ANN to predict R_{Sd} is highly recommended. On the issue of
20 systematic errors as a result of cloud conditions, we certainly expect overestimation or
21 underestimation. The results are discussed in [section 3.2 \(p15, 116 – 127\) \(Figure 9\)](#).

22 4. **FLUXNET site selection.** It was stated that the partition of data into training and
23 validation was randomly selected. However, it’s not clear whether the selected training
24 sites are represent it cover a full range of (from dry to wet) rainfall regimes? For each
25 vegetation type, how much percentage of data is selected to train the model? FLUXNET
26 has more forest sites than grass/shrub sites. Are grass/shrub sites less represented in the
27 training dataset? Following question: is the ANN model sensitive the FLUXNET site
28 selection? This could be evaluated by doing e.g., 10 ensemble of random selection of
29 FLUXNET sites. And check the difference among the resultant 10 ANN models?

1 **Response:** Since this analysis was based on FLUXNET sites distributed across 0-90
2 degrees latitude north and south, the training datasets covers substantial climatic and
3 vegetation variability. The percentage distribution of the training data according to
4 vegetation type was; 23% crops, 31% deciduous broadleaf forest, 10% evergreen
5 broadleaf forest, 20% evergreen needle leaf forest, 8% grassland, 7% shrubs and 1% aquatic
6 as indicated in table S1. The number of grassland and shrubs as indicated were relatively
7 less as compared to the crops and forests sites. **However, biome specific error statistics**
8 **(Fig. 11) indicated the absence of any systematic errors due to vegetation sampling**
9 **with the exception of EBF. Availability of more EBF sites in the training datasets is**
10 **expected to reduce the cloudy sky errors substantially. We have elaborated this**
11 **discussion in the revised manuscript.**

12 We have also performed a sensitivity analysis of R_s -based ANN performance by randomly
13 training ANN with data from different biome combinations and compared ET_d prediction
14 statistics of the different combinations (section 2.6). The results are discussed in section
15 3.5 (p20, l22 – l30 and p21, 11 – 18) (Figure 13).

16 5. **Crop ET.** I think the proposed method might be only suitable for estimating natural
17 terrestrial ecosystem ET . There is large bias of crop ET estimation (Figure 9). That could
18 be due to irrigation? Land management? Those anthropogenic factors (largely alter land
19 surface water budget) is not included in the ANN model and the ET estimation.

20 **Response:** Figure 9 is now Figure 11.

21 Both the current framework and $RsTOA$ -based method of ET_d estimation would be best
22 suited for natural ecosystem as well for the rainfed agroecosystems. In the biome specific
23 ET_d error statistics (Fig. 11), relatively large bias in crop ET is propagated due to the
24 inclusion of irrigated agroecosystems in the validation. Inclusion of daily soil moisture
25 and rainfall in the ANN has shown to improve the R_s -based ET_d prediction only under
26 persistent cloudy-sky conditions. In irrigated agroecosystems, day-to-day variation in soil
27 moisture is not substantial and evapotranspiration is predominantly controlled by the net
28 radiation. Therefore, the inclusion of soil moisture and rainfall in the current ANN
29 framework had not made any improvement in the ET_d prediction statistics in irrigated
30 agroecosystems. Further, having many explanatory variables (e.g., land management,

1 irrigation statistics, anthropogenic factors) to train the ANN, we risk overfitting the model
2 and hence introducing bias. There are now described in the revised manuscript ([section](#)
3 [3.3, p17, 110 – 124](#)).

4 **6. Vegetation control on ET.** The proposed upscaling method is based on the idea that
5 higher available energy (R_s) lead to higher evapotranspiration (ET) (Eqn. 1). It basically
6 assumes that the Bowen ratio does not change during the daytime, so that instantaneous
7 ET/R_s is equal to daily ET/R_s . However, it ignores the important fact that ET is also
8 mediated by vegetation via stomata control. For example, trees and grass have
9 dramatically different stomata density, stomata size. Therefore, their stomata open/closure
10 and its control on water vapor conductance are different.

11 **Response:** This is indeed a very good point and is discussed in [section 4 \(p22, 110 – 124\)](#)
12 of the manuscript. The proposed upscaling method is based on the idea that instantaneous
13 ET/R_s is equal to daily ET/R_s , although it implicitly includes the stomatal controls on ET
14 observations mediated by the vegetation. The cases where ET_i is low due to water stress
15 induced strong stomatal control; low magnitude of ET will also be reflected in upscaling
16 ET_i to ET_d (according to eq. 1). However, to account any carry over effects of the stomatal
17 control on ET_d , inclusion of longwave radiation would likely to improve the scheme.
18 Stomatal control is significantly dependent on the thermal longwave radiative
19 components, and, therefore, the relative proportion of downwelling and upwelling
20 longwave radiation is expected to be a stomatal constraint. However, the availability of
21 longwave radiation measurement stations in the FLUXNET datasets is limited to
22 formulate ANN and evaluate this hypothesis. In general, the stomatal and biophysical
23 constraints are imposed in state-of-the-art thermal remote sensing based ET_i retrieval
24 schemes, and, therefore the ANN framework can be applied to upscale remote sensing
25 based ET_i to ET_d . Also, relatively good performance of the model in semiarid shrubland
26 also indicated the applicability of the method in water stressed ecosystems where stomatal
27 controls are predominant.

28 7. The question is: it is worthwhile to add biome type information in the ANN model? Is it
29 possible to further improve the results (Figure 9) for forest sites by considering biome
30 type information in the ANN model and ET estimates?

1 **Response:** It is not worthwhile to add biome type information in the ANN model. The
2 performance of ANN is principally dependent on atmospheric radiative forcings and less
3 on biome types. To test this hypothesis, we have also performed a sensitivity analysis of
4 R_s -based ANN performance by randomly training ANN with data from different biome
5 combinations and compared ET_d prediction statistics of the different combinations
6 ([section 2.6](#)). The results are discussed in [section 3.5 \(p20, 122 – 130 and p21, 11 – 18\)](#)
7 ([Figure 13](#)).

8 **Minor comments**

9 **Page2**

10 8. L4. a key challenge in mapping regional ET using polar orbiting sensors

11 **Response:** Necessary changes are incorporated ([p2, 13 – 14](#)).

12 9. L6. On the terrestrial surface -> remove

13 **Response:** Removed.

14 10. L8. The approach relies on :: -> remove

15 **Response:** Removed.

16 11. L16. derived from simple mathematical computation -> replace: e.g., solar zenith angle,
17 day length

18 **Response:** Changes are made as suggested ([p2, 113 – 114](#)).

19 12. L20. Based on the measurements from 126 sites -> remove

20 **Response:** Removed.

21 13. L20. Rs -based upscaling produced

22 **Response:** Necessary changes are incorporated ([p2, 117](#))

23

24

1 **Page3**

2 14. L7. ET variability is influenced by (1) available energy received, (2) soil moisture supply
3 and (3) vegetation mediation. I think the third one is missing here. To be complete, the
4 three key factors should all be fairly discussed in the introduction

5 **Response:** Good point. We included the vegetation controls on ET in the introduction ([p3, 111 – 112](#)).

7 15. L9. “Therefore” is not appropriate here, there is no cause-effect relationship here. Better
8 start a new paragraph and discuss the major challenges in Et upscaling

9 **Response:** Done ([p3, 113](#)).

10 **Page4**

11 16. L19. Estimate R_{sd} from any specific time-of-day R_{Si} information. But isn't the value of
12 this study is to predict R_{sd} based at satellite local crossing time (e.g., 10:30, 13:30)?

13 **Response:** The aim of this study is to help develop an approach that would help in the
14 upscaling of ET_i (retrieved at satellite overpass time) to ET_d . The value of this study
15 consists of exploiting R_{Si} information at satellite local crossing time to predict R_{sd} which is
16 not directly retrievable from any polar orbiting satellites, so that the ratio of R_{sd}/R_{Si} can be
17 further used to upscale ET_i to obtain daily ET (ET_d) estimates (in the framework of eqn.
18 1). Currently we are limited to demonstrating with MODIS overpass times (Terra and
19 Aqua), however in case there are new missions in the future with different local overpass
20 time, the method would still be applicable. This description is made explicit in the revised
21 manuscript ([section 2.1, p7, 116 – 122](#)).

22 17. L22. L22. In order -> remove

23 **Response:** Removed ([p4, 128](#)).

24 18. L24. ANN is a non-linear model. Multi-layer perceptron (MLP) is.. These sentences
25 belong to method section.

26 **Response:** The description is now moved in the beginning of [section 2.2 \(p8, 12 – 110\)](#).

27 **Page5**

1 19. L13. Cloudiness is a phenomenon. These sentences belong to discussion section.

2 **Response:** This sentence is moved to [section 3.5 \(p21, l3 – 14\)](#).

3 **Page6**

4 20. L6. Two question: (1) Does Eqn. 1 assume the Bowen ratio is constant during daytime?
5 (2) Does it ignore the night time ET , which could be large when surface wind speed is
6 high?

7 **Response:** According to eqn. 1,

8 $ET_d/ET_i \approx R_{Sd}/R_{Si}$

9 **and**

10 $ET_d/ET_i = EF_d(R_N - G)_d/EF_i(R_N - G)_i$

11 Where EF is the evaporative fraction, R_N is net radiation, and G is ground heat flux.

12 Therefore, eqn. 1 is based on the assumption that shortwave radiation is the principal
13 driver of evaporative flux. Although ET can be limited due to both radiation and water,
14 but in the water limited ecosystems the magnitude of ET_i will also be low due to low soil
15 moisture availability and therefore and upscaling ET_i to ET_d in the framework of eqn. 1
16 may not introduce significant error. The evidence is already seen in Fig. 9 where
17 shrublands showed relatively lower RMSE (despite being water limited) as compared to
18 the forests. We have added this discussion in the revised manuscript ([section 2.1, p6, 114 – 124](#)).

20 (2) The analysis is based on 24-hour period, meaning night time ET contribution is
21 implicitly considered. However, studies have ready shown that the nighttime ET in semi-
22 arid regions contributes only 2 – 5% of the total season ET (Malek, 1992; Tolk, J, Howell,
23 & Evett, 2006), and therefore does not appear to be significant. This is mentioned in
24 [section 2.1 \(p7, 112 – 115\)](#).

25 **Page8**

26 21. L16. In a percentage ratio of 80:15:15. Is this right? Shouldn't be 80:15:5 or 70:15:15?

1 **Response:** The ratio should be 80:15:5, corrections are made in the revised manuscript
2 ([p9, 120](#)).

3 **Page10**

4 22. L9. We first evaluate the efficacy of the ANN method for predicting R_{sd} .

5 **Response:** Necessary changes are incorporated ([p12, 118](#)).

6 23. L12. As obtained following the methodology described in the section 2.1 -> remove

7 **Response:** Necessary changes are incorporated ([p12, 119](#))

8 24. L13. Showing -> including

9 **Response:** Necessary changes are incorporated ([p12, 119](#))

10 25. L14. From the analysis it is apparent that -> remove

11 **Response:** Removed ([p12, 120](#)).

12 **Page 11**

13 26. L1. Figure 5 evaluates the R_{sd_pred} under different level of clear sky transmissivity

14 **Response:** Necessary changes are incorporated in the revised manuscript ([p12, 128](#)).

15 27. L3. What if the ANN model includes “clear sky transmissivity, would model performance
16 under cloudy sky condition be improved?

17 **Response:** We do not think so, because including clear sky transmissivity could make the
18 modeling framework biased towards clear sky cases only.

19 28. L16. Using R_{sd_pred}/R_{si} as a scaling factor following eq. 1 -> remove

20 **Response:** Necessary changes are incorporated ([p13](#)).

21 **Page 12**

22 29. L1. Figure 7 compares ET_{d_pred} against ET_{d_obs} for different level of daily. The overall
23 RMSE, MAPE

1 **Response:** Necessary changes are incorporated ([p14, 11](#)).

2 30. L4. Given that the overestimation is a systematic, is it possible to eliminate it or reduce it?
3 The overestimation was due to the fact that during the specific time slot of interest (e.g.,
4 11:30) the sky is clear while the sky is cloudy during other times. However, there could be
5 another opposite case that sky is cloudy at e.g., 11:30 but clear at other times. It will
6 probably lead to an underestimation of R_{Sd_pred} , and consequently underestimation of
7 ET_{d_pred} . I am wondering why the latter is not the case at least in Figure 7.

8 **Response:** This is a very good argument. With the current framework of ANN, this
9 systematic overestimation cannot be eliminated. However, as demonstrated in Fig 11, with
10 the inclusion of daily rainfall and soil moisture in the ANN model, such overestimation
11 tendency could be reduced ([p15, 11 – 19](#)).

12 Regarding R1's argument on finding underestimation of ET_d from 1100 hr cloudy sky ET_i
13 upscaling in a predominant clear day, such cases were also found in τ_3 category ([Fig. 7](#))
14 where clouds of data points clearly falling significantly below the 1:1 line, thus showing
15 substantial underestimation of ET_d . We have included this discussion in the revised
16 manuscript ([p14, 111 – 115](#)).

17 31. L14. higher errors in ET_{d_pred} can be expected. Is there a way to overcome this problem?

18 **Response:** One of the probable ways to overcome the errors in cloudy sky is to
19 incorporate daily rainfall and soil moisture or information of cloud cover in the ANN.
20 This is now demonstrated in the revised manuscript and related discussions are included
21 in ([p15, 11 – 111](#)).

22 32. L24. Again, biome specific results are related to the clear-sky issue. Tropical evergreen
23 broadleaf forests have high ET, water tends to re-cycle locally and generate rainfall. It's
24 reasonable to see that cloudy sky condition is more frequent at tropical evergreen
25 broadleaf forest than e.g., at grass land.

26 **Response:** Agreed. This point is added in the discussion of the revised manuscript. This
27 discussion is now moved in [section 3.3 \(p16, 129 – 130; p17, 11 – 124\)](#).

1 33. L27. ET estimations at cropland were much worse than grass. It that because e.g.,
2 irrigation? Land management? Or any other anthropogenic factors that are not considered
3 in the ANN model? Page 13.

4 Response: Yes, the farm management practice especially irrigation might have impact on
5 the output for example in a case where irrigation was carried out for three consecutive
6 days yet the sky conditions were consistently cloudy would present a challenge.
7 Necessary discussions are in section 3.3 (p17, 116 – 118).

8 **Page 13**

9 34. L20. Based on Table 2, Figure 11, R_s TOA method seems successful. Under clear sky
10 condition, it was even better than the proposed R_s method. Further, over longer time scale
11 (annually), there is no big difference between R_s TOA and R_s .

12 Response: Agreed and discussed also in the manuscript. As shown in Table 2, relatively
13 lower RMSE of R_s TOA for atmospheric transmissivity class above 0.75 reveals that
14 under pristine clear sky conditions R_s TOA can be successfully used to upscale ET_i .
15 However, one of the main reasons for the differences in RMSE between R_s and R_s TOA
16 method for daily transmissivity above 0.75 could be due to the fact that if ET_i upscaling is
17 performed from a cloudy instance for a predominantly clear sky day, then such RMSE
18 difference between the two different upscaling methods is expected. These results also
19 showed the probability of a hybrid ET_i upscaling method by combining R_s -method (for
20 transmissivity between zero to 0.5) and R_s TOA-method (for transmissivity greater than
21 0.5). However this hypothesis needs to be tested further. Discussions are included in
22 section 3.3 (p18, 123 – 130, p19, 11 – 12) of the revised manuscript.

23 **Page 16**

24 35. L1. Briefly define what R_s TOA-based method is, what is R_s method.

25 **Response:** R_s -TOA-based method is the upscaling method based on R_s TOA and R_s
26 method is the method based on R_s . The meaning R_s TOA and R_s were earlier defined in
27 the manuscript; please see Page 4 (11 – 15). We have further expanded this in the
28 conclusion section (p21).

1 36. L4. ET_{d,pred} are defined early in the manuscript, consider the summary as an independent
2 section. Better not to use these acronyms, or re-define it.

3 **Response:** Agreed, necessary changes are made (p22, l4 – 15)

4 37. L21-25. This paragraph belongs to results & discussion section.

5 **Response:** This paragraph is now moved to section 3.3 (p19, l28 onwards)

6

7

8

9

10

11

12

13

14

15

16

17

18

19

20

21

1 **Reviewer 2 (R2)**

21. How do you pick the training sites? Will the vegetation type and climate type (seasonal
3 climate) have any effect on your trained ANN algorithm? Given that Fluxnet sites at least in
4 N. America are mostly forest sites, will that have any potential impact on your trained ANN?’

5 **Response:** The training sites were randomly selected with a representative across latitude 0-
6 90° North and South at 10 degree interval. The potential impact of vegetation on ANN
7 training is now described in section 3.5 (p21 – p22) through a sensitivity analysis of ANN
8 performance to different training scenarios.

92. I think a paragraph on R_s and factors affecting R_s is missing from the paper. This is necessary
10 to justify your choice of inputs for your ANN.

11 **Response:** Necessary discussions are incorporated in section 2.1 (p7, l23 – l31).

123. Please include discussion on why the method performs poorly over cropland (Figure 9)

13 **Response:** The probable reason of the poor ET_d prediction in the croplands could be due to the
14 effects of irrigation that is unaccounted in ET_i upscaling. Since the upscaling factor is based
15 on the ratio of instantaneous to daily shortwave radiation, the impacts due to irrigation cannot
16 be capture, and higher errors can be expected. We have added this description in the revised
17 manuscript (section 3.3, p17, l11 onwards).

184. As discussed in lines 25-27, R_{sd} and cloudiness are directly related. ANN has no input related
19 to cloudiness. However, you argue that you assess the performance of ANN under cloudy sky
20 condition based on simple cloudiness index. Please elaborate on this and include discussion in
21 the paper. Can you use Precipitation or the index of cloudiness as an input to your ANN?

22 **Response:** The daily cloudiness index was estimated as the ratio between observed R_{sd} and
23 extraterrestrial shortwave radiation to assess the performance of the ANN under variable
24 cloud conditions (p11, l1 – l7).

25 The use of daily precipitation and soil moisture can be an improvement in the ANN model.
26 To test this hypothesis, we have included an analysis using a subset of sites over which daily
27 soil moisture and rainfall data were available. The results are shown in Figure 9. Necessary
28 descriptions are added in section 3.2 (p15, l1 – l27).

15. Since vegetation plays an important role in Evapotranspiration, it would be interesting to
2 compare different scaling methods against the type of vegetation as well (in graphs or figures)

3 **Response:** We have added a comparison statistics of two different scaling methods (Rs-based
4 and RsTOA-based) across different vegetation types ([Fig. 11](#)) and the results are explained in
5 [section 3.3 \(p16, l29 – l30; p17, l1 – l10\)](#).

6

7

8

9

10

11

12

13

14

15

16

17

18

19

20

21

22

1 **Reviewer 3 (R3)**

2 **R3 overall view on the manuscript**

3 (1) "I don't see the point of upscaling ET_i to ET_d for days where instantaneous observations in
4 the optical domain are not available from satellite platforms: instantaneous ET_i estimates are
5 usually produced with instantaneous data in the optical domain, typically Thermal Infrared
6 data, and are therefore not computed for low transmissivities, airborne platforms excepted.

7 **Response:** We disagree with R3 here. R3 should be aware that there are established ET
8 modeling schemes that explicitly considers cloudy sky cases e.g., ALEXI model (Anderson et
9 al., 2007). Also to overcome the cloudy sky ET_i retrieval in optical domain, modeling
10 schemes have been suggested to combine both optical and microwave remote sensing (Kustas
11 et al., 1998). Therefore, R3's argument on ignoring ET_i computation for low atmospheric
12 transmissivities is not substantiated.

13 (2) Days with low instantaneous (10AM, 1:30PM) transmissivities should be left out of the
14 study i.e. the study should restrict to clear sky conditions from either MODIS cloud mask or,
15 better, geostationary information (the CERES algorithm mentioned here). I therefore doubt
16 that there is any use of the method for "Remote sensing applications" as mentioned in the title,
17 except for UAV applications."

18 **Response:** We do not agree for the reasons mentioned in the previous response. The bigger
19 picture here is focussing on the conceptual development of a robust method for upscaling ET_i
20 to ET_d from remote sensing platforms across variable sky conditions that can be used for
21 operational purpose. For remote sensing applications, the greatest challenge is the ET_i
22 upscaling in cloudy conditions, which the proposed method is able to tackle relatively better
23 as compared to R_s TOA or EF based method (Table 2). R3's inclination on clear sky cases and
24 rejecting the present method could only be applicable in predominantly pristine clear sky. We
25 have already demonstrated this fact in Table 3 that when the temporal frequency of the data is
26 coarse (8-day to annual), there is practically no difference between R_s and R_s TOA based
27 upscaling. But this does not deviate from the central message that R_s -based method appears to
28 perform better when atmospheric transmissivity is between zero to 0.5.

1 (3) Even for clear sky conditions the ANN method shows worse performances than the
2 classical method based on the sole earth-sun geometrical parameters.

3 **Response:** It is surprising to see R3's constrained judgement on the ANN method. R3's
4 comment on worse performance appears to be an over-statement if we consider Table 2,
5 where MAPD between R_s and R_{sTOA} differs by only 2-3 percent at transmissivity level
6 above 0.5. Contrarily, we see this as an opportunity for a hybrid modeling scheme to upscale
7 ET_i across variable sky conditions by using ANN for transmissivity level of zero to 0.5 and
8 using R_{sTOA} method for transmissivity level above 0.5. Also, as mentioned in the
9 manuscript, if upscaling is done from cloudy instances for a predominantly clear day, the
10 discrepancy between ANN and R_{sTOA} method seems to be obvious. This problem can also
11 be overcome by including daily rainfall and soil moisture in the ANN framework, which is
12 now demonstrated in the revised manuscript ([section 3.2, p15, 11 – 127](#)).

13 (4) ETR between 2 successive clear sky days is an interpolation problem (which could be also
14 treated using ANN) which needs to be tackled also.

15 **Response:** This manuscript discussed about a potential ET_i upscaling strategy to convert
16 satellite retrieved ET_i to ET_d . We do not foresee any interpolation problem that needs to be
17 tackled.

18 **R3 main comments**

19 1. **I also share the main concern with R1** about Energy Balance Closure: Lack of EBC
20 should not be overlooked and is simple to correct for FLUXNET sites; it could explain the
21 poor performance of the Evaporative Fraction method. Disregarding EBC is a major
22 methodological flaw of the paper.

23 **Response:** We have included an additional analysis on the performance of the proposed
24 ET_i upscaling method after closing the surface energy balance in the FLUXNET sites in
25 [section 3.4 \(p20, 14 – 121\)](#). All the existing literatures have already demonstrated the poor
26 performance of evaporative fraction based ET upscaling methods despite EBC closure.

27 2. **As criticized also by R1**, Crops and semi-arid or even dry sub humid sites are
28 underrepresented in the FLUXNET database; this should be more carefully commented. It
29 adds up to my concern above about the practical application of the method: TIR based

1 daily ETR computation algorithms are particularly needed for water use monitoring in
2 water depleted environments, much less for natural vegetation in temperate climates.'

3 **Response:** Under-representation of crops and semi-arid sites in the FLUXNET database does
4 not necessarily limit the practical applications of this method. As already described in the
5 response of R1 that the relatively high errors in ET_d in croplands might be due to neglecting
6 the irrigation effects in the ANN and inclusion of daily soil moisture and rainfall in the ANN
7 might improve the predictive power of the modeling framework particularly over the irrigated
8 agroecosystem. However, the performance of the method in the semi-arid shrublands appear
9 to be promising (Fig. 11) and therefore the method seems to be credible under water-stressed
10 environment also. This approach is equally important for natural systems e.g., in the Amazon
11 basin or in the forest ecosystems where significant hydrological and climatological
12 projections are emphasizing the role of ET_d to understand the resilience of natural ecosystems
13 in the spectre of hydro-climatological extremes (Harper et al., 2014; Kim et al., 2012). These
14 are discussed in section 3.3 (P17, 17 – 131; p18, 11 – 13).

15 3. Are the validation and the training datasets from different years? It seems to me that this is
16 a requirement to use the method for future applications.'

17 **Response:** Yes, the training and validation datasets are from different years. The validation
18 was performed over independent sites also which are clearly delineated in Fig. 3.

19 4. What is the true added value of the ANN for future operational applications of the
20 upscaling algorithm, say for an operational satellite product? This aspect, although the
21 original motivation of the paper, is somewhat overlooked in the discussion section.'

22 **Response:** Yes, the true added value of the ANN is for an operational daily ET_d
23 product from polar satellites. Currently, the polar Earth orbiting satellites provide us with
24 ET_i only. However, for most hydrological and ecosystem modeling applications, ET_d is
25 needed. Therefore, for studies that will opt to apply the Rs method as a scaling algorithm,
26 R_{sd} will be easily available for any measurement of R_{Si} by the satellite using the ANN. We
27 have made this point explicit in the conclusion (section 4) of the revised manuscript (p22,
28 128 – 131; p23, 11).

1 5. For cloudy conditions the ETR upscaling method using instantaneous solar radiation as
2 part of the training (even from another site) performs slightly better than that based on the
3 sole TOA solar radiation: is it mostly due to the fact that the ANN adds information on
4 actual incoming radiation obtained at a "nearby" FLUXNET location?"

5 **Response:** This is not true. From Table 2, it is clearly seen that the ET upscaling
6 method based on shortwave radiation has outperformed the TOA-based method
7 under cloudy to moderately clear sky conditions when atmospheric transmissivity is
8 between zero to 0.5. However under the clearest sky, the shortwave radiation based
9 method showed relatively higher RMSE than the RsTOA-based method. If the ANN
10 adds information on actual incoming radiation obtained at a "nearby" FLUXNET location,
11 then we would expect the ANN to produce lower RMSE for all the classes of atmospheric
12 transmissivity. These statistics rather strengthens the fact that if upscaling is done from a
13 cloudy instance for a predominant clear sky day, higher errors can be expected from the
14 shortwave radiation based upscaling method. Discussions are already included in the
15 revised manuscript (p18, l12 – l18; p19, l1 – l2).

16 **R3 Minor comments**

17 6. In introduction one should add a review of which upscaling support variables can be
18 derived from remote sensing data directly, which can be obtained indirectly from either RS
19 data or any other distributed routinely produced data and those not obtainable from remote
20 sensing or other distributed operational datasets.

21 **Response:** Good point. We have added necessary description in the introduction (p4, l28 –
22 l31; p5, l1 – l3) and also in section 2.1 (p7, l23 – l31) of the revised manuscript.

23 7. How do you manage night-time conditions?"

24 **Response:** The answer to this question is already provided in the response of R1 (p7, l12 –
25 l15).

26 8. Move P5L1-4 to the end of this section and precise the variables fed by ANN upfront
27 there.

28 **Response:** Agreed. The objectives are moved at the end of the introduction.

1 9. It is not clear, why there is a testing dataset and a separate validation dataset within the
2 training dataset?

3 **Response:** The ANN algorithm is designed to validate its performance for any given
4 training which in most cases should be sufficient for validating the network. However to
5 ensure the network is robust, we further test the generated network with independent
6 dataset. We have mentioned this this in the revised manuscript (p9, l20 – l23).

7 10. P9L5: ‘Why use transmissivity rather than the ration between actual and theoretical
8 clearsky radiations to separate the various cloudiness bins? (in order at least to separate
9 winter conditions with lower clear sky transmissivity from summer conditions).

10 **Response:** We disagree. Transmissivity gives the actual sky conditions and should be used
11 to classify differential cloudiness levels. The estimation of theoretical clear-sky radiation is
12 based on the assumption of clear sky transmissivity (which is typically 0.75). Separating
13 sky conditions based on actual and theoretical clear sky radiation might produce baffling
14 results in cases when actual radiation is higher than the theoretical clear sky radiation.

15 11. P14L10: “would likely”: this can be checked, is it the case?

16 **Response:** Corrected (p18, l11).

17 12. P13L12: “reasonable” > “reasonably”

18 **Response:** Corrected (p16, l7).

19

20

21

22

23

24

25

1 **Upscaling instantaneous to daily evapotranspiration using**
2 **modelled daily shortwave radiation for remote sensing**
3 **applications: an Artificial Neural Network approach**

4 Loise Wandera^{1,2}, Kaniska Mallick¹, Gerard Kiely³, Olivier Rouspard⁴, Matthias Peichl⁵,
5 Vincenzo Magliulo⁶

6 ¹Remote Sensing and Ecohydrological Modeling, Dept. ERIN, Luxembourg Institute of Science and
7 Technology, Belvaux, Luxembourg

8 ²Water Resources, Dept. ITC, University of Twente, Enschede, Netherlands

9 ³Hydrology, Micrometeorology & Climate Investigations, HYDROMET Research Group, University College
10 Cork, Ireland

11 ⁴CIRAD, UMR Ecology and Soils, Montpellier, France

12 ⁵Forest Landscape Biogeochemistry, Dept. Swedish University of Agricultural Sciences Umeå, Sweden

13 ⁶Consiglio Nazionale delle Ricerche, ISAFOM, Ercolano, Napoli, Italy

14

15

16 Correspondence to: Kaniska Mallick (Phone: +352 275888425; email:
17 kaniska.mallick@gmail.com); Loise Wandera (email: loise.wandera@list.lu);

18

19

20

21

22

23

24

1 **Abstract**

2 Upscaling instantaneous evapotranspiration retrieved at any specific ~~time of day~~~~time-of-day~~ (ET_i) to daily evapotranspiration (ET_d) is ~~a key challenge in mapping regional ET using polar orbiting sensors. a key challenge in regional scale vegetation water use mapping using polar orbiting sensors.~~ Various studies have unanimously cited the short wave incoming radiation (R_s) to be the most robust reference variable explaining the ratio between ET_d and ET_i ~~on the terrestrial surfaces~~. This study aims to contribute in ET_i upscaling for global studies using the ratio between daily and instantaneous incoming short wave radiation (R_{sd}/R_{si}) as a factor for converting ET_i to ET_d . ~~The approach relies on the availability of R_{sd} measurements that in many cases is hindered if not by cost but due to the environmental conditions such as cloudiness.~~

12 This paper proposes an artificial neural network (ANN) machine learning algorithm first to predict R_{sd} from R_{si} followed by using the R_{sd}/R_{si} ratio to convert ET_i to ET_d across different terrestrial ecosystem. Using R_{si} and R_{sd} observations from multiple sub-networks of FLUXNET database spread across different climates and biomes (to represent inputs that would typically be obtainable from remote sensors during the overpass time) in conjunction with some astronomical variables (~~derived from simple mathematical computatione.g., solar zenith angle, day length, exoatmospheric shortwave radiation etc.~~), we developed ANN model for reproducing R_{sd} and further used it to upscale ET_i to ET_d . The efficiency of the ANN is evaluated for different morning and afternoon ~~time of day~~~~time-of-day~~, under varying sky conditions, and also at different geographic locations. ~~Based on the measurements from 126 sites, we found R_s -based upscaled ET_d to produce~~ ~~produced~~ a significant linear relation ($R^2 = 0.65$ to 0.69), low bias (-0.31 to -0.56 $MJ\ m^{-2}\ d^{-1}$) (appx. 4%), and good agreement (RMSE 1.55 to 1.86 $MJ\ m^{-2}\ d^{-1}$) (appx. 10%) with the observed ET_d , although a systematic overestimation of ET_d was also noted under persistent cloudy sky conditions. ~~Inclusion of soil moisture and rainfall information in ANN training was found reduced the systematic overestimation tendency on overcast days.~~ An intercomparison with existing upscaling method at daily, 8-day, monthly, and yearly temporal resolution revealed a robust performance of the ANN driven R_s -based ET_i upscaling method and was found to produce lowest RMSE under cloudy conditions. ~~Sensitivity analysis revealed variable sensitivity of the method to biome selection and high ET_d prediction errors in forest ecosystems are primarily~~

1 | associated with greater rainfall and clouds. The overall methodology appears to be promising
2 | and has substantial potential for upscaling ET_i to ET_d for field and regional scale
3 | evapotranspiration mapping studies using polar orbiting satellites.

4 | **Key Words:** Evapotranspiration, upscaling, artificial neural networks, short wave radiation,
5 | rainfall, soil moisture, FLUXNET

6 | **1 Introduction**

7 | Satellite-based mapping and monitoring of daily regional evapotranspiration (ET hereafter)
8 | (or latent heat flux, λE) is considered as a key scientific concern for multitudes of applications
9 | including drought monitoring, water rights management, ecosystem water use efficiency
10 | assessment, distributed hydrological modelling, climate change studies, and numerical
11 | weather prediction (Anderson et al., 2015; Senay et al., 2015; Sepulcre-Canto et al., 2014). ET
12 | variability during the course of a day is influenced by changes in the radiative energy being
13 | received at the surface (Brutsaert & Sugita, 1992; Crago, 1996; Parlange & Katul, 1992), and
14 | also due to soil moisture variability particularly in the water deficit landscapes, and also due
15 | to the stomatal regulation by vegetation.

16 | Therefore, one of the fundamental challenges in regional ET modelling using polar orbiting
17 | sensors satellites involves the upscaling of instantaneous ET retrieved at any specific time-of-
18 | daytime time-of-day (ET_i hereafter) to daily ET (ET_d hereafter). For example, ET_i retrieved
19 | from LANDSAT, ASTER and MODIS sensors typically represent ET_i at a single snapshot of
20 | 1000, 1030 and 1330 hrs local times, which needs to be upscaled to daily timescales for
21 | making this information usable to hydrologists and water managers (Cammalleri et al., 2014;
22 | Colaizzi et al., 2006; Ryu et al., 2012; Tang et al., 2013).

23 | In order to accommodate the temporal scaling challenges encountered by remote sensing
24 | based ET models, techniques have been proposed and applied by various researchers to
25 | upscale ET_i to ET_d . These include: (1) the constant evaporative fraction (EF) approach which
26 | assumes a constant ratio between λE and net available energy ($\phi = R_n - G$, R_n is the net
27 | radiation and G is the ground heat flux) during daytime [$EF = \lambda E / (R_n - G)$] (Gentine et al.,
28 | 2007; Shuttleworth et al., 1989), (2) constant reference evaporative fractions (EF_r) method
29 | where the ratio of ET_i between a reference crop (typically grass measuring a height of 0.12 m

1 in an environment that is not water limited) and an actual surface is assumed to be constant
2 during daytime, allowing ET_d to be estimated from the daily EF_r (Allen et al., 1998; Tang et
3 al., 2013), (3) constant global shortwave radiation method (R_S) where R_S is the reference
4 variable at the land surface and it is assumed that the ratio of daily to instantaneous shortwave
5 radiation (R_{Sd} and R_{Si}) values (i.e., R_{Sd}/R_{Si}) determines ET_d to ET_i ratio (Jackson et al., 1983;
6 Cammalleri et al., 2014), and (4) constant extra-terrestrial radiation method where the exo-
7 atmospheric shortwave radiation (R_{STOA}) is the reference variable and the ratio of
8 instantaneous to daily R_{STOA} (R_{SiTOA} and R_{SdTOA}) is assumed to determine the ratio of ET_d
9 to ET_i (Ryu et al., 2012; Van Niel et al., 2012). These methods have been reviewed and
10 compared in different studies with the view of identifying the most robust ET_i to ET_d
11 upscaling approach based on different data sets, time integrals and varying sky conditions
12 (Cammalleri et al., 2014; Ryu et al., 2012; Tang et al., 2013, 2015; Van Niel et al., 2012; Xu et
13 al., 2015).

14 Based on the previous studies, we find that the R_{STOA} approach performed consistently good
15 at lower temporal resolution namely eight-day to monthly scales (Ryu et al., 2012; Van Niel
16 et al., 2012) as well as under clear-sky conditions (Cammalleri et al., 2014), whereas the R_S
17 approach was identified as the most preferred method for ET_i to ET_d conversion at a higher
18 temporal scale i.e. daily timescale in addition to under variable sky conditions (Cammalleri et
19 al., 2014; Chávez et al., 2008; Colaizzi, et al., 2006; Xu et al., 2015). Although the EF_r -based
20 method produced comparable ET_d estimates as the R_S -based method, however the dependence
21 of EF_r estimates on certain variables (e.g., daily net available energy; ϕ and wind speed) and
22 the difficulty to characterise them at the daily scale from single acquisition of polar orbiting
23 satellites (Tang et al., 2015) makes it a relatively less attractive method. Furthermore the EF_r -
24 based method appeared to consistently underestimate ET_d in all these studies.

25 The motivation of the current work is built on the conclusions of Colaizzi et al. (2006),
26 Chávez et al. (2008), Cammalleri et al. (2014), and Xu et al. (2015) that the ratio of the
27 instantaneous to daily R_S incident on land surface is the most robust reference variable
28 explaining the ratio between ET_d and ET_i among all the tested methods. This work aims to
29 contribute in ET_i upscaling by first developing a method for estimating R_{Sd} from any specific
30 time-of-day R_S information (R_{Si}) and further using R_{Sd}/R_{Si} ratio as a factor for converting ET_i
31 to ET_d . We develop an artificial neural network (ANN) machine learning algorithm

(McCulloch & Pitts, 1943) in order to estimate R_{Sd} . Although net radiation (R_N) is more closely associated with ET , but R_S constitutes 80-85% of R_N (Mallick et al., 2015). Also from remote sensing perspective, R_{Si} is relatively easily retrievable irrespective of the sky conditions (Wang et al., 2015; Lopez and Battles, 2014), and its relationship to R_{Sd} is primarily governed by cloudiness (cloud fraction, cloud optical depth) and astronomical variables (e.g., solar zenith angle, day length, R_{STOA} etc.). Given the information of cloudiness is also obtainable from remote sensing, we consider R_S to be a robust variable to explore ET upscaling. ANN is a non-linear model which works by initially understanding the behaviour of a system based on a combination of a given number of inputs and subsequently is able to simulate the system when fed with an independent set of inputs of the same system. ANN is an approach that has been successfully used in estimating global solar radiation in many sectors and more so in the field of renewable energy (Ahmad et al., 2015; Hasni et al., 2012; Lazzus et al., 2011). Multi layer perceptron (MLP) is one of the ANN architectures commonly used as opposed to other statistical methods, makes no prior assumptions concerning the data distribution, has ability to reasonably handle non-linear functions and reliably generalise independent data when presented (Gardner & Dorling, 1998; Khatib, Mohamed, & Sopian, 2012; Wang, 2003).

Even though this study is intended for remote sensing application, we tested the method using meteorological and surface energy balance flux measurements from eddy covariance (EC) system at the FLUXNET (Baldocchi et al., 2001) sites mainly for the purpose of temporal consistency. However, we evaluate the performance in consideration with overpass time of polar orbiting satellites commonly used in operational ET mapping namely MODIS and LANDSAT. By choosing to use data distributed over different ecosystems and climates zones, we are faced with two problems : (1) changing cloud conditions across ecosystems, (2) varying energy balance closure (EBC) requirements for the fluxes in different ecosystems (Foken et al., 2006; Franssen et al., 2010; Mauder & Foken, 2006; Wilson et al., 2002).

Cloudiness is a phenomenon that significantly influences the reliability of a model to predict incoming solar radiation as they are directly related to each other. Currently, information on cloudiness is obtainable from geostationary meteorological satellites, at hourly to 3-hourly time steps e.g., from the Clouds and Earth's Radiant Energy System (CERES), the International Satellite Cloud Climatology Project–Flux Data (ISCCP-FD), and Global Energy

1 and Water cycle Experiment Surface Radiation Budget (GEWEX-SRB). The CERES
2 algorithm uses cloud information from MODIS onboard both Terra and Aqua platforms and
3 combines it with information from geostationary satellites to accurately capture the diurnal
4 cycles of clouds. In this study, cloudiness is not included in the list of variables used to
5 estimate R_{Sd} due to inconsistency in spatial resolution of data to match with the other
6 predictive variables used. Including cloudiness holds a great potential in improving the ANN
7 R_{Sd} predictions due to their direct relationship (Mallick et al., 2015). However, we assess the
8 performance of the ANN under cloudy sky conditions based on simple cloudiness index
9 computations as adopted from previous works (Baigorria et al., 2004). The EBC problems
10 have been reported to vary across landscapes due to management practices, climate, seasons
11 and plant functional type characteristics (Foken et al., 2006). In this study, in order to test the
12 robustness of the proposed method, we initially disregard the site specific EBC problems and
13 assume that the systematic bias of fluxes fall within the same range across entire FLUXNET
14 database used.

15 The objectives of the present study are: (1) using a ANN with Multilayer Perceptron (MLP)
16 architecture to predict R_{Sd} based on R_{Si} satellite observations, (2) applying R_{Sd}/R_{Si} ratio as a
17 scaling factor to upscale ET_i to ET_d ~~based on R_{Sd}/R_{Si} ratio~~ under all sky conditions, and (3)
18 comparing the performance of proposed R_S -based ET_i upscaling method with R_{STOA} and EF -
19 based ET_i upscaling methods across a range of temporal scales, biomes and variable sky
20 conditions.

21 2 Methodology

22 2.1 Rationale

23 The presented method of ET upscaling from any specific time of day to daytime average evaporative fluxes is based on the assumption of self-preservation of
24 incoming solar energy (i.e., shortwave radiation) as proposed by Jackson et al. (1983).
25

$$26 \quad ET_d \approx ET_i \frac{R_{Sd}}{R_{Si}} \quad (1)$$

27 Where, ET_d is the daily average evapotranspiration in $W \text{ m}^{-2} \text{ MJ} \text{ m}^{-2} \text{ d}^{-1}$, ET_i is the
28 instantaneous evapotranspiration at any instance during daytime in $W \text{ m}^{-2}$, R_{Si} and R_{Sd} are the

values of shortwave radiation recorded at any instance and the daily average having units W m^{-2} . Daily total ET_d and R_{Sd} is expressed in $\text{MJ m}^{-2} \text{d}^{-1}$ by using standard conversion from Watts to Mega Joules. Following Jackson et al. (1983) and Cammalleri et al. (2014), we hypothesized that the mean diurnal variation of ET for any particular day scales with the mean diurnal variation of R_S . The justifications are: (a) R_S is the principal driver that controls sub-daily ET variability unless there is substantial diurnal asymmetry in cloudiness or abrupt change in sub-daily soil moisture between morning and afternoon. (b) Under thick cloudy conditions, ET scales with R_S . Under clear sky conditions ET also scales with R_S and both are in phase if sufficient soil moisture is available at the surface. (c) Phase difference between R_S and ET are commonly found under soil moisture deficit conditions in clear-sky days. However, the magnitude of clear-sky ET_i in water deficit conditions is also be very low, which will lead to substantially low ET_i/R_{Si} ratio, and would unlikely to introduce any uncertainty in ET_i to ET_d upscaling in the framework of eq. (1).

For any remote sensing studies using polar orbiting satellites, although the retrieval of ET_i and R_{Si} has been standardised (Tang et al., 2015; Huang et al., 2012; Polo et al., 2008; Laine et al., 1999), but, estimating R_{Sd} and ET_d from R_{Si} and ET_i are still challenging. Presently, upscaling R_{Si} to R_{Sd} is primarily based on the clear sky assumption, i.e., for the entire daytime integration period, the sky remains cloud-free (Bisht et al., 2005; Jackson et al., 1983). However, the clear-sky assumption is not always appropriate for upscaling remote sensing based R_{Si} and hence ET_i because the sky conditions during a specific ~~time-of-day~~ ~~time-of-day~~ may be clear whereas the other part of the day might be cloudy. Under such conditions, the clear-sky assumption of ET_i upscaling will lead to substantial overestimation of ET_d in cloudy conditions. Hence reliable estimates of all-sky (i.e., both clear and cloudy) R_{Sd} would greatly improve the ET_d estimates in the framework of eq. (1). Given the unavailability of a definite method to directly estimate all-sky R_{Sd} from R_{Si} information, here we proposed a simple method to upscale R_{Si} to R_{Sd} using ANN. This method uses the observations of both R_{Sd} and R_{Si} from all the available FLUXNET sites in conjunction with some ancillary variables to build the ANN as described in section 2.2. A schematic diagram of the ANN method is given in Fig. 1. The analysis is based on 24-hour period, meaning night time ET contribution is implicitly considered. However, studies have already shown that the nighttime

1 ET in semi-arid and sub-humid regions contributes only 2 – 5% of the total season ET (Malek,
2 1992; Tolk et al., 2006), and therefore does not appear to be significant.

3 The overarching aim of this study is to develop an approach that would help in the upscaling
4 of ET_i (retrieved at satellite overpass time) to ET_d . Additional value of this study also consists
5 of exploiting R_{Si} information at satellite local crossing time to predict R_{Sd} which is not directly
6 retrievable from any polar orbiting satellites, so that the ratio of R_{Sd}/R_{Si} can be further used to
7 upscale ET_i to obtain ET_d estimates. Currently we are limited to demonstrating with MODIS
8 satellite overpass times (Terra and Aqua), however for the future missions with different local
9 overpass time, the method would still be applicable.

10 In any natural ecosystem, R_S on a particular day is primarily influenced by the cloud
11 (especially cloud cover fraction and optical thickness) (Mallick et al., 2015; Hildebrandt et al.,
12 2007), latitude, season, and time-of-day. Therefore, R_{Sd} on any specific day is expected to be a
13 function of R_{Si} (as a representative of R_S and cloudiness factors), solar zenith angle
14 (representing latitude, season, time-of-day), day length (representing latitude and season), and
15 R_{SiTOA} (representing latitude, season, time-of-day). Besides, atmospheric aerosols also
16 interact with R_S and absorb some of the radiation particularly in the urban areas. Considering
17 the applications of ET_i to ET_d modeling in the natural ecosystems, we include R_{Si} , R_{SiTOA} ,
18 R_{SdTOA} , solar zenith angle and day length for R_{Sd} (and subsequently ET_d) prediction.

19 2.2 Development of Artificial Neural Network (ANN)

20 ANN is a non-linear model which works by initially understanding the behaviour of a system
21 based on a combination of a given number of inputs and subsequently is able to simulate the
22 system when fed with an independent set of inputs of the same system. ANN approach has
23 been successfully used in estimating global solar radiation in many sectors and more so in the
24 field of renewable energy (Ahmad et al., 2015; Hasni et al., 2012; Lazzús et al., 2011). Multi-
25 layer perceptron (MLP) is one of the ANN architectures commonly used as opposed to other
26 statistical methods, makes no prior assumptions concerning the data distribution, has ability to
27 reasonably handle non-linear functions and reliably generalise independent data when
28 presented (Gardner & Dorling, 1998; Khatib, Mohamed, & Sopian, 2012; Wang, 2003). In the
29 present study, MLP was chosen as it has been widely used in many similar studies and cited
30 to be a better alternative as compared to the conventional statistical methods (Ahmad et al.,

1 2015; Chen et al., 2013; Dahmani et al., 2016; Mubiru & Banda, 2008). The MLP is
 2 composed of 5 neurons in the input layer, 1 output layer and 10 hidden layers (Fig. 2). The
 3 input layer neurons are made up of instantaneous incoming short wave radiation (R_{Si}),
 4 instantaneous exo-atmospheric shortwave radiation (R_{SiTOA}), daily exo-atmospheric
 5 shortwave radiation (R_{SdTOA}), solar zenith angle (θ_Z), and day length (L_D) as the predictor
 6 variables whose values are initially standardized to range between -1 to 1. The choice of the
 7 inputs is intentionally limited to the variables that cannot only be acquired by measurements
 8 from meteorological stations but also derived from simple astronomical computations (Ryu et
 9 al., 2012) mainly to help minimize on the spatial distribution problem (as described earlier in
 10 the introduction) that is often linked to ground weather stations. In the MLP processing, the
 11 input layer directs the values of each input neuron x_i ($i = 1, 2, 3, \dots, n$) into each neuron (j) of
 12 the hidden layers. In the hidden layer, x_i is multiplied by a weight (w_{ij}) followed by a *bias* (b_j)
 13 assigned for each hidden layer also is applied. The weighted sum (eq. (2)) is fed into a
 14 transfer function. In this work a tangent sigmoid (TANSIG) function is used (eq. (3)) in the
 15 hidden layer while in the output layer a PURELIN function is applied (eq. (4)) to give a single
 16 output value which is the predicted daily shortwave radiation (R_{Sd_pred}). PURELIN is a linear
 17 neural transfer function used in backpropagation network. It calculates a layer's output from
 18 its net input. The function generates outputs between zero and 1 as the neuron's net input goes
 19 from negative to positive infinity. The training of the ANN is completed by a regression
 20 analysis being performed internally by the algorithm between the target variable i.e. the
 21 observed and predicted daily shortwave radiation (R_{Sd_obs} and R_{Sd_pred}).

$$x_j = \sum_{i=1}^n w_{ij} y_i b_j \quad (2)$$

$$y_j = \frac{2}{(1 + \exp(-2x_j) - 1)} \quad (3)$$

$$y_j = X_i(\text{PURELIN}) \quad (4)$$

22 Bayesian regularization algorithm was chosen for the optimization process because it is able
 23 to handle noisy datasets by continuously applying adaptive weight minimization and can
 24 reduce or eliminate the need for lengthy cross-validation that often leads to overtraining and
 25 overfitting of models (Burden and Winkler, 2009).

1 **2.3 Datasets**

2 Daily and half-hourly data on R_S (W m^{-2}), R_{STOA} , net radiation (R_n , W m^{-2}), latent heat flux
3 (λE , W m^{-2}), sensible heat flux (H , W m^{-2}) and ground heat flux (G , W m^{-2}) measured by the
4 FLUXNET (Baldocchi et al., 2001) eddy covariance network were used. A total of 126 sites
5 from the years 1999 to 2006 distributed between latitude 0-90 degrees north and south of the
6 equator were used for the present analysis. The data sites covered a broad spectrum of
7 vegetation functional types and climatic conditions and a list of the sites are given in Table S1
8 in the supplementary section.

9 Among 126 sites, 85 sites were used for training and remaining 41 sites were used for
10 validation. Partition of the data into training and validation was randomly selected regardless
11 of the year. These translated into 194 and 86 yearly data for the respective sample. A global
12 distribution of the data sites is shown in Fig. 3. From the training dataset, three samples were
13 internally generated by the algorithm i.e., training datasets, validation datasets, and a testing
14 dataset in a percentage ratio of 80:15:~~15-5~~ respectively. The ANN algorithm is designed to
15 validate its performance for any given training which in most cases should be sufficient for
16 validating the network. However to ensure the network is robust, we further test the generated
17 network with independent dataset. Considering the equatorial crossing time of different polar
18 orbiting sensors like LANDSAT, ASTER, and MODIS Terra-Aqua, unique networks were
19 generated for different time of day from morning to afternoon, and thus we had a total of 8
20 networks to represent potential satellite overpass times between 1030 to 1400 hours using 30
21 minutes interval as the closest reference time for each hour. The generated networks were
22 then applied to an independent validation data set.

23 **2.4 Intercomparison of ET_i upscaling methods**

24 An intercomparison of three different ET_i upscaling methods is performed with the
25 homogeneous datasets to assess their relative performance across a range of temporal scales
26 and variable sky conditions. These are: (a) R_S -based upscaling method, where ANN predicted
27 R_{Sd} is used in conjunction with observed R_{Si} to predict ET_d using eq. (1).
28 (b) The exo-atmospheric irradiance method (Ryu et al., 2012) where the reference variable is
29 R_{STOA} .

$$R_{sd}TOA = S_{sc} \left[1 + 0.033 \cos \left(\frac{2\pi t_d}{365} \right) \right] \cos \theta_z \quad (5)$$

$$SF_{RTOA} = \frac{R_{sd}TOA}{R_{Si}TOA} \quad (6)$$

$$ET_d = ET_i SF_{RTOA} \quad (7)$$

Where S_{sc} is the solar constant (1360 W m^{-2}), t_d is the day of year (DoY), and θ_z is the solar zenith angle. The performance of the R_s method is also compared with two other existing E_t upscaling methods:

(a) the EF -based method (Cammalleri et al., 2014), where reference variable is the net available energy (ϕ) (i.e., $R_n - G$).

$$SF_{EF} = \frac{\lambda E}{R_n - G} \quad (8)$$

$$ET_d = 1.1(R_n - G)_d SF_{EF} \quad (9)$$

Where SF_{EF} is the EF -based scaling factor, $(R_n - G)_d$ is the daily net available energy.

(b) The exo-atmospheric irradiance method (Ryu et al., 2012) where the reference variable is R_s TOA.

$$R_{sa}TOA = S_{se} \left[1 + 0.033 \cos \left(\frac{2\pi t_a}{365} \right) \right] \cos \beta \quad (6)$$

$$SF_{RTOA} = \frac{R_{sa}TOA}{R_{st}TOA}$$

$$ET_a = ET_i SF_{RTOA}$$

Where S_{se} is the solar constant (1360 W m^{-2}), t_a is the day of year, and β is computed solar zenith angle.

We tested the performance of the three upscaling algorithms for all possible sky conditions assumed to be represented by daily atmospheric transmissivity (τ_d) (eq. 710) namely (i)

1 0.25 $\geq \tau \geq 0$ (τ_1 , hereafter), (ii) 0.5 $\geq \tau \geq 0.25$ (τ_2 , hereafter) (iii) 0.75 $\geq \tau \geq 0.5$ (τ_3 , hereafter), and (iv)
 2 1 $\geq \tau \geq 0.75$ (τ_4 , hereafter), respectively. We use daily τ because it indicates the overall sky
 3 condition throughout a day.

$$\tau_d = \frac{R_{Sd}}{R_{Sd}TOA} \quad (710)$$

4 R_{Sd} and $R_{Sd}TOA$ are daily shortwave radiation and the exo-atmospheric shortwave radiation in
 5 $\text{MJ m}^{-2} \text{ d}^{-1}$ (converted from W m^{-2}).

6 2.5 Statistical error analysis

7 The relative performance of the ANN and three upscaling methods is evaluated using
 8 statistical indices generated namely: coefficient of determination (R^2), mean absolute
 9 percentage error (MAPE), root mean square error (RMSE), mean absolute percentage error
 10 (MAPE), coefficient of determination (R^2), index of agreement (IA), and bias. ET_d estimates
 11 using the respective upscaling coefficients were compared with measured ET_d .

$$R^2 = 1 - \frac{\sum_{i=1}^n (P_i - O_i)^2}{\sum_{i=1}^n (O_i)^2} \quad (811)$$

$$RMSE = \sqrt{\frac{\sum_{i=1}^n (O_i - P_i)^2}{n}} \quad (912)$$

$$MAPE = \frac{1}{n} \sum_{i=1}^n \frac{|O_i - P_i|}{n} * 100 \quad (1013)$$

$$IA = \frac{\sum_{i=1}^n (P_i - O_i)^2}{\sum_{i=1}^n (|P_i - O_i| + |O_i - P_i|)^2} \quad (1114)$$

$$Bias = \frac{\sum_{i=1}^n (P_i - O_i)}{n} \quad (1215)$$

1 Where, n is the number of data points; o_i and p_i are daily observed and estimated R_{Sd} or ET_d ,
2 respectively. \bar{O} was the mean value of observed R_{Sd} or ET_d .

3 **2.6 Sensitivity of ANN training and validation**

4 Given the majority of the FLUXNET sites represent forest biomes and the distribution of EC
5 sites over non-forest biomes are proportionately lower as compared to the forests, we
6 performed a sensitivity analysis of the ANN-based approach by assessing the error statistics
7 (R^2 and RMSE) of predicted ET_d for different scenarios of ANN training. Three case studies
8 were generated: (a) Case1, where ANN was trained by including data randomly from the
9 forests and ET_d validation was done in non-forest biomes (i.e., grassland, crops and
10 shrublands); (b) Case2, where ANN was trained by including data randomly from the non-
11 forest biomes and predicted ET_d was evaluated in forest biome; (c) ANN was trained by using
12 data randomly from equal proportions of forest and non-forest biomes, and ET_d validation was
13 also done in forest and non-forest biomes. Each individual case was replicated 10 times and
14 an ensemble mean statistics of predicted ET_d is reported in section 3.5.

15 **3 Results and discussion**

16 **3.1 Testing the performance of predicted R_{Sd}**

17 Given that the performance of ET_d upscaling depends on the soundness of R_{Sd} estimation, we
18 first evaluate the efficacy of the ANN method for predicting R_{Sd} . feel some justification to
19 demonstrate the efficacy of the ANN method for predicting R_{Sd} Figure 4 summarises the
20 statistical results of predicted R_{Sd} (R_{Sd_pred} , hereafter) as obtained following the methodology
21 described in the section 2.1, showing including all the site-year average R^2 , RMSE, IA, and
22 MAPE values for eight different time of day time-of-day upscaling time slots. From the
23 analysis it is apparent that tThe RMSE of R_{Sd_pred} from forenoon upscaling time slots. From the
24 analysis it is apparent that tThe RMSE of R_{Sd_pred} from forenoon upscaling time slots. From the
25 analysis it is apparent that tThe RMSE of R_{Sd_pred} from forenoon upscaling time slots. From the
26 analysis it is apparent that tThe RMSE of R_{Sd_pred} from forenoon upscaling time slots. From the
27 analysis it is apparent that tThe RMSE of R_{Sd_pred} from forenoon upscaling time slots. From the
28 analysis it is apparent that tThe RMSE of R_{Sd_pred} from forenoon upscaling time slots. From the
29 analysis it is apparent that tThe RMSE of R_{Sd_pred} from forenoon upscaling time slots. From the

1 Figure 5 (a, b) evaluates R_{Sd_pred} statistics under different level of atmospheric transmissivity
2 (τ) ($0.25 \geq \tau \geq 0$, $0.5 \geq \tau \geq 0.25$, $0.75 \geq \tau \geq 0.5$, and $1 \geq \tau \geq 0.75$) shows the two-dimensional scatters
3 between R_{Sd_pred} versus R_{Sd_obs} for different levels of τ with an overall RMSE of 1.81 and 1.83
4 MJ m⁻² d⁻¹ for the forenoon and afternoon upscaling respectively. Table 1 and Fig. 5 clearly
5 show an overestimation tendency of the current method under persistent cloudy sky
6 conditions (τ_1), whereas the predictive capacity of the ANN model is reasonably strong with
7 increasing atmospheric clearness. The RMSE of R_{Sd_pred} for different τ class from forenoon
8 upscaling varied between 0.62 to 2.45 MJ m⁻² d⁻¹, with MAPE, R² and IA of 9.2 to 53%, 0.67
9 to 0.98, and 0.67 to 0.95, respectively (Table 1). For the afternoon upscaling these statistics
10 were 0.89 to 2.4 MJ m⁻² d⁻¹ (RMSE), 2.4 to 52% (MAPE), 0.65 to 0.98 (R²), and 0.67 to 0.95
11 (IA) (Table 1).

12 The overestimation of R_{Sd_pred} at low values of τ is presumably associated with varying levels
13 of cloudiness during the daytime. Since R_{Sd_pred} depends on the magnitude of R_{Si} , L_D , θ_Z ,
14 R_{SiTOA} , and R_{SdTOA} , there will be a tendency of overestimating R_{Sd_pred} on partly cloudy days if
15 R_{Si} at a specific ~~time of day~~ ~~time-of-day~~ is not affected by the clouds (L_D , θ_Z , R_{SiTOA} , and
16 R_{SdTOA} are not influenced by the clouds).

17 3.2 Evaluation of predicted ET_d based on R_{Sd_pred}

18 Figure 6 summarises the statistical results of predicted ET_d (ET_{d_pred} , hereafter) ~~using~~
19 ~~R_{Sd_pred}/R_{Si} as a scaling factor following eq. 1~~ for eight different ~~time of day~~ ~~time-of-day~~
20 slots. Upon statistical evaluation, all the cases showed significantly linear relationship
21 between ET_{d_pred} and observed ET_d (ET_{d_obs} , hereafter). The RMSE of ET_{d_pred} from forenoon
22 upscaling varied from 1.67–1.84 MJ m⁻² d⁻¹, with MAPE, R², IA varying between 30%–34%,
23 0.62–0.68, and 0.77–0.80, respectively (Fig. 6). For the afternoon upscaling, these statistics
24 varied between 1.5–1.6 MJ m⁻² d⁻¹, 29%–30%, 0.67–0.71, and 0.80 (Fig. 6). These results also
25 indicate that the error statistics were nearly uniform and the accuracy of ET_{d_pred} varied only
26 slightly when integration was done from different ~~time of day~~ ~~time-of-day~~ hours between
27 1030 to 1400 h. These typical error characteristics can greatly benefit the ET_d modelling using
28 polar orbiting data with varying overpass times between 1030 to 1400 hours. This also opens
29 up the possibility to use either forenoon satellite (e.g., MODIS Terra, LANDSAT, ASTER
30 etc.) or afternoon satellite (i.e., MODIS Aqua) to upscale ET_i to ET_d . Following R_{Sd} , here also

1 we restricted our analysis to the two different ~~time of day~~^{time-of-day} (1100h and 1330h)
2 representing Terra and Aqua overpass times.

3 Figure 7 (a and b) ~~compares ET_{d_pred} against ET_{d_obs} for different level of daily~~^{shows the two}
4 ~~dimensional scatters between ET_{d_pred} versus ET_{d_obs} for different levels of daily τ . The with~~
5 ~~an~~ overall RMSE, MAPE, and R^2 ~~of were~~ 1.86 and 1.55 MJ m⁻² d⁻¹, 31% and 36%, 0.65 and
6 0.69 for the forenoon and afternoon upscaling, respectively. As seen in Fig. 7, there is a
7 systematic overestimation of ET_{d_pred} relative to the tower observed values for low range of τ
8 (i.e., cloudy sky). It is important to realise that, unlike ET_{d_obs} , ET_{d_pred} might be an outcome
9 of ET_i instances when the sky was not overcast, i.e., the sky conditions might be clear at
10 specific ~~time of day~~^{time-of-day} but can be substantially overcast for the remainder of the
11 daytime. As a result, any bias in the daily shortwave radiation prediction (R_{Sd_pred}) will result
12 in biased ET_{d_pred} according to eq. 1, and the omission of non-clear sky conditions at any
13 particular time of daytime would tend to lead to $ET_{d_pred} > ET_{d_obs}$ for generally overcast days.
14 ~~However, there could be another opposite case that sky is cloudy at e.g., 1100 hr but clear at~~
15 ~~other times. This will probably lead to an underestimation of R_{Sd_pred} , and consequently~~
16 ~~underestimation of ET_{d_pred} . Such cases were also found in τ_3 categories in Fig. 7 where~~
17 ~~clouds of data points clearly falling significantly below the 1:1 line, thus showing substantial~~
18 ~~underestimation of ET_{d_pred} . Since ET_{d_obs} are the integrations of multiple ET_i measurements,~~
19 such conditions could be conveniently captured in the observations which were not possible
20 in the current framework of ET_{d_pred} . Therefore, when upscaling was done under clear skies at
21 nominal acquisition time for generally overcast days, higher errors in ET_{d_pred} can be expected
22 (Cammalleri et al., 2014) and vice-versa. We examined this cloudy sky overestimation pattern
23 in greater detail by evaluating the error statistics in ET_{d_pred} for four different levels of daily τ
24 categories (Fig. 8).

25 ~~The-s~~Statistical evaluation of ET_{d_pred} for different classes of daily τ ~~(estimated as the ratio~~
26 ~~between daily observed R_{Sd} and R_{Sd_TOA})~~ indicates the tendency of higher RMSE and low R^2
27 in ET_{d_pred} under the persistent cloudy-sky conditions (τ_1), while the performance of ET_{d_pred} is
28 reasonably good with increasing atmospheric clearness (τ_2 , τ_3 , and τ_4) (Fig. 8). The RMSE of
29 ET_{d_pred} for different τ class from forenoon upscaling varied between 1.09 to 2.96 MJ m⁻² d⁻¹,
30 with MAPE, R^2 and IA of 25 to 75%, 0.38 to 0.79, and 0.71 to 0.82, respectively. For the

1 afternoon upscaling, these statistics were 0.98 to 2.02 MJ m⁻² d⁻¹ (RMSE), 24 to 87%
2 (MAPE), 0.40 to 0.68 (R²), and 0.71 to 0.77 (IA).

3 To probe into detail of the high errors under persistent cloudiness conditions, a new ANN was
4 trained by introducing daily precipitation (P) and soil moisture (SM) information (along with
5 R_S , R_{STOA} , θ_Z , and L_D) assuming that the inclusion of these two variables might improve the
6 predictive power of R_S -based ANN. In the new ANN, we used data from the sites where
7 coincident measurements of P and SM were available along with R_S and ET , and validated
8 ET_d predictions of the new ANN on independent sites. The analysis revealed 34% reduction
9 in RMSE (from 3.28 to 2.88 MJ m⁻² d⁻¹), 16% reduction in MAPE (from 90 to 76%), and 49%
10 reduction in mean bias (0.76 to 0.39 MJ m⁻² d⁻¹) for persistent cloudy-sky cases (i.e., τ_1
11 scenarios) from 1100 hr upscaling. However, no significant improvements in ET_{d_pred} were
12 evident for τ_2 , τ_3 , and τ_4 and also for any of the τ classes from the afternoon (1330 hr)
13 upscaling (Fig. 9). ET_d is generally controlled by radiation and soil moisture availability.
14 Under the radiation controlled conditions, ET_d is generally not limited due to soil moisture
15 and 70 – 75% of the net radiation is contributed to ET_d . Therefore, R_S -based method of ET_i
16 upscaling is expected to perform reasonably well unless the upscaling is performed from a
17 clear sky instance for a predominantly overcast or rainy day. However, from Fig. 9 is it
18 apparent that the inclusion of cloud information (cloud fraction, cloud optical thickness) in
19 R_S -based ANN would substantially reduce ET_{d_pred} errors when upscaling is performed from a
20 clear sky instance for a predominantly overcast day and vice-versa. Improvements of ET_{d_pred}
21 error statistics by including daily P and SM (as an indicator of cloudiness) is also suggestive
22 to the relevance of such approach as a future improvement of the current framework, which is
23 expected to reduce the systematic error under overcast conditions. However, the cloud
24 information available from alternative sources e.g., from the Clouds and Earth's Radiant
25 Energy System (CERES), the International Satellite Cloud Climatology Project–Flux Data
26 (ISCCP-FD), and Global Energy and Water cycle Experiment Surface Radiation Budget
27 (GEWEX-SRB) are available at coarse spatial resolution (100 km²) and combining these
28 information with EC tower measurements to train ANN could also introduce additional errors
29 due to the spatial scale mismatch, is therefore out of scope of the present study.

30 Figure 10 shows the time series comparisons between observed ET_d and ET_{d_pred} for four
31 different stations representing different latitude bands of both the Northern (Sweden) and

1 Southern (Brazil, Australia, and South Africa) hemispheres. These reveal that the temporal
2 dynamics of ET_d is in general consistently captured by the proposed method throughout year.
3 In Br_SP1, relatively less seasonality was found in both observed and predicted ET_d . This is
4 because SP1 is a tropical site having an annual rainfall of 850–1100 mm most of which is
5 evenly distributed between March to end of September. The peaks in ET_d values during the
6 beginning of year and October onwards coincided with the periods of increased R_s , and
7 ET_{d_pred} could reasonably capture the observed trends during both rainy and non-rainy
8 periods. Similarly the low ET_d pattern (0.1 to 2 MJ m⁻² d⁻¹) in the hot arid climate of South
9 Africa (Za-Kru) could also be ~~reasonable~~reasonably captured in ET_{d_pred} (Fig. 10). ET_{d_pred} in
10 the other Southern hemisphere (AU-Tum) and Northern hemisphere (SE-Fla) sites have
11 shown distinct seasonality (high summer and low winter ET_d) coinciding with the observed
12 ET_d patterns.

13 **3.3 Comparison with existing ET upscaling methods**

14 ET_{d_pred} from R_s -based method was intercompared with two other upscaling schemes (R_sTOA
15 and EF) over 41 FLUXNET validation sites for two different ~~time-of-day~~time-of-day~~time-of-day~~,
16 1100h and 1330h, the statistics of which are given in Table 2. This comparison was also
17 carried out according to different τ classes as defined in section 2.2.3.

18 From Table 2 it is apparent that the R_s -based method has generally produced relatively low
19 RMSE (1.21 to 1.99 MJ m⁻² d⁻¹) and MAPE (23 to 50%) as well as relatively high IA (0.72 to
20 0.84) as compared to R_sTOA and EF -based upscaling methods. The EF -based upscaling
21 method appears to systematically underestimate ET_d for both forenoon and afternoon as
22 evident from high negative bias compared to the other two methods (Table 2). On comparing
23 R_s and R_sTOA methods, R_s -based method performed relatively better than the R_sTOA scheme
24 for low magnitude of τ (i.e., under predominantly cloudy-sky). However, the results suggest
25 comparable performance of R_sTOA -based approach under clear sky conditions which are
26 reflected in lowest RMSE (1.09 and 1.13 MJ m⁻² d⁻¹) in ET_{d_pred} as compared to the other τ
27 classes. In general, all the schemes performed relatively better from the afternoon upscaling as
28 compared to the morning upscaling (as evidenced in higher R^2 and lower bias) (Table 2)
29 which is in agreement with the findings from Ryu et al. (2012). [Due to their comparable error](#)

1 statistics, an intercomparison of R_s and R_sTOA -based methods of ET_d upscaling was also
2 carried out across different biomes.

3 Biome specific evaluation of R_s -based $ET_{d\ pred}$ (Fig. 11) revealed lowest RMSE and highest
4 R^2 both in the grassland (GRA) (0.68 to 1.14 MJ $m^{-2} d^{-1}$; 0.53 to 0.79) and shrubland (SH)
5 (0.66 to 1.76 MJ $m^{-2} d^{-1}$; 0.60 to 0.82) whereas the RMSE was comparatively high over the
6 tropical evergreen broadleaf forests (EBF) (1.41 to 2.02 MJ $m^{-2} d^{-1}$) and deciduous broadleaf
7 forests (DBF) (1.94 to 2.55 MJ $m^{-2} d^{-1}$). Similar evaluation with R_sTOA -based method
8 revealed the lowest RMSE and highest R^2 in the grassland (0.64 to 1.14 MJ $m^{-2} d^{-1}$; 0.61 to
9 0.84), and highest RMSE in EBF, DBF, and evergreen needleleaf forests (ENF) (1.57 to 2.05
10 MJ $m^{-2} d^{-1}$, 1.2 to 2.25 MJ $m^{-2} d^{-1}$ and 0.93 to 4.02 MJ $m^{-2} d^{-1}$) (Fig. 11c and 11d). Higher
11 $ET_{d\ pred}$ errors in forests are related to the predominant cloudy-sky issue as described earlier.
12 Tropical evergreen broadleaf forests (and forests in general) have high ET , water tends to re-
13 cycle locally and generate rainfall. Therefore, cloudy sky conditions are more frequent at
14 tropical evergreen broadleaf forest and other forests types than at grassland and shrublands. In
15 the biome specific $ET_{d\ pred}$ error statistics (Fig. 11), relatively large bias in crop $ET_{d\ pred}$ is
16 introduced due to the inclusion of irrigated agroecosystems in the validation. In irrigated
17 agroecosystems, day-to-day variation in soil moisture is not substantial and ET_d is
18 predominantly controlled by the net radiation. Therefore, the inclusion of soil moisture in the
19 current ANN framework is unlikely to improve $ET_{d\ pred}$ statistics in the irrigated
20 agroecosystems. Further having many explanatory variables (e.g., land management,
21 irrigation statistics, anthropogenic factors) to train the ANN, we risk overfitting the model and
22 hence introducing bias. It is also evident that both R_s and R_sTOA -based method of ET_d
23 estimation would be better suited for natural ecosystem e.g., in the Amazon basin or in the
24 forest ecosystems where significant hydrological and climatological projections are
25 emphasizing the role of ET_d to understand the resilience of natural ecosystems in the spectre
26 of hydro-climatological extremes (Harper et al., 2014; Kim et al., 2012). The performance of
27 the method in the semi-arid shrublands appear to be promising (Fig. 11) and therefore the
28 method seems to be credible under water-stressed environment also.

29 Given this analysis was based on FLUXNET sites distributed across 0-90 degrees latitude
30 north and south, the training datasets covers substantial climatic and vegetation variability.
31 The percentage distribution of the training data according to vegetation type was; 23% crops,

31% deciduous broadleaf forest, 10% evergreen broadleaf forest, 20% evergreen need leaf forest, 8% grassland, 7% shrubs and 1% aquatic as indicated in table S1. The number of grassland and shrubs as indicated were relatively less as compared to the crops and forests sites. However, biome specific error statistics (Fig. 11) indicted the absence of any systematic errors due to vegetation sampling with the exception of EBF. Availability of more EBF sites in the training datasets is expected to reduce the cloudy-sky errors substantially, due to the assimilation of more cloud information into the R_s -based ANN training.

The tendency of positive bias in ET_{d_pred} from both R_s and R_sTOA in clear skies from afternoon upscaling is partly explained by the fact that, during the afternoon the values of both R_s and R_sTOA reached maximum limit and dominates their daily values (Jackson et al., 1983). The post afternoon rate of reduction in ET does not coincide with the shortwave radiation due to stomatal controls on ET , and the total water flux from morning to afternoon (0700h to 1300h) is generally greater than the total water flux from post afternoon (1500h onwards) till sunset. Therefore multiplying 1330h ET_i with high magnitude of R_{Sd}/R_{Si} or $R_{Sd}TOA/R_{Si}TOA$ ~~might would likely~~ lead to an overestimation of ET_{d_pred} in the clear sky days.

Since extraterrestrial shortwave radiation is not affected by the clouds, ET_{d_pred} from R_sTOA performed comparably with the R_s -based ET_{d_pred} with increasing atmospheric clearness (i.e., for the higher levels of daily τ). However, increased differences in the RMSE of ET_{d_pred} between R_s and R_sTOA upscaling in the predominantly cloudy days indicates that more deviations can be expected in ET_{d_pred} from these two different method of upscaling under principally overcast conditions (Tang et al., 2013). This happens because the ratio of $R_{Sd}TOA/R_{Si}TOA$ is not impacted by the clouds and the magnitude of this ratio becomes markedly different from R_{Sd}/R_{Si} ratio in the presence of clouds, which leads to the differences in ET_{d_pred} between them. The R_s -based method is relatively efficient to discriminate the impacts on ET by R_{Sd}/R_{Si} due to the clouds. The generally good performance of R_s -based method and comparable error statistics with R_sTOA -based ET_d estimates are consistent with the findings of Cammalleri et al. (2014) and Van Niel et al. (2012). As shown in Table 2, relatively lower RMSE of R_sTOA -based ET_{d_pred} for atmospheric transmissivity class above 0.75 reveals that under pristine clear sky conditions R_sTOA can be successfully used to upscale ET_i . However, one of the main reasons for the differences in RMSE between R_s and R_sTOA method for daily transmissivity above 0.75 could be due to the fact that if ET_i upscaling is performed from a

1 cloudy instance for a predominantly clear sky day, then such RMSE difference between the
2 two different upscaling methods is expected. These results also revealed the probability of a
3 hybrid ET_i upscaling method by combining cloud information or SM and P in R_S -method (for
4 transmissivity between zero to 0.5) and R_S TOA-method (for transmissivity greater than 0.5).
5 However this hypothesis needs to be tested further.

6 The systematic ET_d underestimation by EF -based upscaling method and nearly similar pattern
7 of bias from two different ~~time-of-daytime-of-day~~ upscaling (Table 2) further points to
8 the fact that the concave-up shape of EF during daytime (Hoedjes et al., 2008; Tang et al.,
9 2013) will tend to underestimate ET_d if EF is assumed to be conservative during the daytime.
10 EF remains conservative during the daytime under extremely dry conditions when ET_d is
11 solely driven by deep layer soil moisture. The systematic underestimation of ET_d from EF -
12 based upscaling method corroborates with the results reported by other researchers
13 (Cammalleri et al., 2014; Delogu et al., 2012; Gentine et al., 2007; Hoedjes et al., 2008)
14 which suggests that the self-preservation of EF is not generally achieved, and this systematic
15 underestimation of ET_d can be partially compensated if EF -based ET_i upscaling is done from
16 morning 0900h or afternoon 1600h ~~time-of-daytime-of-day~~.

17 We further resampled ET_d (both predicted and observed) from daily to 8-day, monthly, and
18 annual scale, and statistical metrics from the three different upscaling methods at three
19 different temporal scales are shown in Fig. 12 and Table 3. Averaging ET_d at 8-day, monthly
20 and annual scale substantially reduced the RMSE to the order of 60 to 70% for all the three
21 upscaling methods. The R_S -based upscaled ET_d from morning and afternoon showed reduction
22 in RMSE from 1.79 MJ to 0.57 MJ and 1.74 MJ to 0.51 MJ from daily to annual ET ,
23 respectively. For the other two upscaling method these statistics varied from 1.85 and 1.89 MJ
24 to 0.62 and 0.53 MJ (R_S TOA method), and 2.16 and 1.33 MJ to 2.20 and 1.31 MJ (EF
25 method) (Fig. 12 and Table 3). The impacts of daily cloud variability might have smoothed
26 out in 8-day, monthly and annual scale which led to reduced RMSE and higher correlation
27 between $ET_{d,pred}$ and $ET_{d,obs}$. Nearly similar error statistics in $ET_{d,pred}$ from both the morning
28 and afternoon upscaling also substantiates the findings of Ryu et al. (2012) and greatly
29 stimulate the use of either morning satellite (i.e., Terra) or after satellite (i.e., Aqua) to upscale
30 ET_i to ET_d or 8-day mean ET_d .

1 The principal limitation of the approach is the dependence of ET_d and R_{Sd} on single snapshot
2 of ET_i and R_{Si} . Although hourly R_S data from geostationary satellite are becoming available;
3 but these are available as sectorial products (i.e. for particular continents) instead of full
4 global coverage. Ongoing efforts to develop geostationary based data by merging multiple
5 geostationary satellites tend to overcome this limitation.

6 **3.4 Impact of energy balance closure on ET_d _{pred}**

7 FLUXNET EC sites have long been identified to be prone to surface energy budget
8 imbalance, which might lead to ($\pm 20\%$) to ($\pm 40\%$) under measurement of latent heat fluxes.
9 In order to assess the impacts of surface energy balance (SEB) closure on current ET_d
10 prediction, we further compared the error statistics of R_S -based ET_d _{pred} (Table 4) for both
11 'closed' and 'unclosed' surface energy balance datasets. These are the subsets of the data
12 where all the four SEB components (λE , sensible heat flux, ground heat flux, and net
13 radiation) were available and SEB was closed by the Bowen ratio closure method (Foken,
14 2006). Table 4 revealed substantially low RMSE (10 to 60%), R^2 (8 to 100%) and MAPE (1
15 to 75%) in ET_d _{pred} when ET_i upscaling is done by 'unclosed' SEB. A consistently high
16 positive mean bias (0.63 to 3.83) in ET_d _{pred} with 'closed' SEB was also noted (Table 4).
17 Although, various methods exist to close the surface energy balance, but, the impact of
18 various SEB closure methods on ET_d _{pred} statistics is beyond the scope of the current study. It
19 is also important to mention that in the satellite based ET_i retrieval, net available energy is
20 partitioned into ET and sensible heat flux with the implicit assumption of SEB closure.
21 Therefore, application of the current ANN framework is expected not to impact the remote
22 sensing based ET_i to ET_d upscaling. However, for the validation of remote sensing based ET_d
23 retrievals, surface energy balance fluxes from eddy covariance measurements need to be
24 closed.

25 **3.5 Sensitivity of ANN derived ET_d _{pred} to biome selection**

26 A sensitivity analysis of ANN derived R_S -based ET_d _{pred} revealed variable sensitivity of the
27 ANN framework to the biome selection. The coefficient of determination (R^2) varied between
28 0.71 to 0.84 and RMSE between 0.96 to 2.10 MJ m⁻² d⁻¹ across three different scenarios of
29 ANN training and validation (Fig. 13). However, RMSE was found to be relatively high in
30 forests in Case2, where ANN was trained by using the data from crops, grasslands and

1 shrublands only. For the Case1 and Case3, no substantial difference was noted (Fig. 13). This
2 therefore revealed the fact that the inclusion of forests in ANN training leads to lower errors
3 in ET_d over non-forest biomes, although the reverse scenario is not likely to be true. Since
4 forests generally have high ET , water recycling tends to be more over the forests which
5 produces substantial rainfall, variable atmospheric water vapor, associated cloudiness, and
6 radiation. Cloudiness is a phenomenon that significantly influences the reliability of a model
7 to predict incoming solar radiation as they are directly related to each other. Therefore, when
8 R_s -based ANN is trained with data from forests, the model assimilates information on a
9 diverse range of radiative forcings which broaden their applicability in other biomes. This
10 also emphasizes the fact that the performance of such ANN-based approach is primarily
11 sensitive to their training over a broad spectrum of atmospheric conditions.

12 4 Summary and Conclusions

13 Given the significance of ET_d in remote sensing based water resource management from polar
14 orbiting satellites, this study developed and evaluated a temporal upscaling method for
15 estimating ET_d from different ~~time-of-day~~ instantaneous ET (ET_i)
16 measurements with the assumption that the ratio between daytime to instantaneous shortwave
17 radiation (R_{sd}/R_{si}) is the predominant factor governing ET_d/ET_i ratio. However, since R_{sd} is
18 not directly measurable from the polar orbiting satellites, we trained an ANN with the
19 FLUXNET observations of R_{si} and R_{sd} , and validated the model to predict R_{sd} over
20 independent sites, followed by using R_{sd}/R_{si} ratio for converting ET_i to ET_d ~~we first developed~~
21 ~~a robust ANN-based method to upscale R_{si} to R_{sd} followed by using the ratio of R_{sd}/R_{si} to~~
22 ~~further upscale ET_i to ET_d~~ . The overarching goal of this study is to provide an operational and
23 robust ET_i upscaling protocol for estimating ET_d from any polar orbiting satellite. The datasets
24 used for the ANN model development covers a wide range of biome, climate, and variable
25 sky conditions. Therefore, we assume the R_{sd} prediction from ANN to capture a broad
26 spectrum of radiative forcing, which is also reflected in the independent validation of R_{sd} and
27 ET_d (Fig. 5, Fig. 7, Table 2). However, the performance of this model for satellite retrieval of
28 R_{sd} (from R_{si}) is dependent on the accuracy of R_{si} retrieval (Loew et al., 2016). Also, the
29 distribution of sites over the tropics, Africa, and South East Asia are poor, and more sites over
30 these regions are expected to make the ANN model performance more robust.

1 Based on measurements from 126 flux tower sites, we found R_s -based upscaled ET_d to
2 produce a significant linear relation ($R^2 = 0.65$ to 0.69), little bias (-0.31 to -0.56 MJ $m^{-2} d^{-1}$)
3 (appx. 4%), and good agreement (RMSE 1.55 to 1.86 MJ $m^{-2} d^{-1}$) (appx. 10%) with the
4 observed ET_d . While the exoatmospheric shortwave radiation driven ET_i upscaling method
5 (i.e., R_sTOA -based) appeared to produce slightly lower RMSE (10% lower) under cloud-free
6 conditions (Table 2), global shortwave radiation driven method (i.e., R_s -based method)
7 demonstrates more robust performance and was found to be better under cloudy conditions.
8 Despite R_s -based method yielded relatively better overall accuracy in ET_d prediction (i.e.,
9 ET_{d_pred}) statistics when compared with the R_sTOA and evaporative fraction based (EF-based)
10 method, statistical analysis of ET_{d_pred} accuracy of different temporal upscaling methods (as
11 discussed in section 3.3) suggests that R_s and R_sTOA to produce commensurate results under
12 coarse temporal resolutions (Table 3). Therefore, at the coarse temporal scale (8-day and
13 above), any of these two methods (R_s and R_sTOA) can be used for ET_i to ET_d upscaling.

14 The proposed upscaling method is based on the idea that instantaneous ET/R_s is equal to daily
15 ET/R_s , although it implicitly includes the stomatal controls on ET observations mediated by
16 the vegetation. The cases where ET_i is low due to water stress induced strong stomatal
17 control; low magnitude of ET will also be reflected in upscaling ET_i to ET_d (according to eq.
18 1). However, to account for any carry over effects of the stomatal control on ET_d , inclusion of
19 longwave radiation would likely to improve the scheme. Stomatal control is significantly
20 dependent on the thermal longwave radiative components, and, therefore, the relative
21 proportion of downwelling and upwelling longwave radiation is expected to be a stomatal
22 constraint. However, the availability of longwave radiation measurement stations in the
23 FLUXNET datasets is limited to formulate ANN and evaluate this hypothesis. In general, the
24 stomatal and biophysical constraints are imposed in state-of-the-art thermal remote sensing
25 based ET_i retrieval schemes, and, therefore the ANN framework can be applied to upscale
26 remote sensing based ET_i to ET_d . Also, relatively good performance of the model in semiarid
27 shrubland also indicated the applicability of the method in water stressed ecosystems where
28 stomatal controls are predominant.

29 Among all the upscaling method tested, R_s -based method carries maximum information on
30 the cloudiness and produced generally lowest RMSE, low bias (Table 3), and, therefore,
31 overall the preferably robust scaling mechanism (at the daily scale) among all the other

1 methods tested. The true added value of the ANN is for an operational ET_d product from polar
2 satellites. Currently, the polar Earth orbiting satellites provide us with ET_i only. However, for
3 most hydrological and ecosystem modeling applications, ET_d is needed. Therefore, for studies
4 that will opt to apply R_s -based method as a scaling algorithm, R_{sd} will be easily available for
5 any measurement of R_{Si} by the satellite using the ANN. However, upscaling large-area
6 satellite-based ET_i by using retrieved R_{Si} would require accurate R_{Si} retrieval techniques,
7 which are currently commonplace (Ahmad et al., 2015; Boulifa et al., 2015; Dahmani et al.,
8 2016; Hasni et al., 2012; Li, Tang, Wu, & Liu, 2013) to support regional scale hydrological
9 applications. Of the two other upscaling methods, R_sTOA could be easily applied over large
10 areas, had lower errors than EF , had second best RMSE, and overall lowest bias among the
11 two. We conclude that using modelled R_s to upscale ET_i at daily scale appears to be viable for
12 large-area hydrological remote sensing applications from polar orbiting satellites irrespective
13 of any sky conditions.

14 ~~The principal limitation of the approach is the dependence of ET_d and R_{sd} on single snapshot~~
15 ~~of ET_i and R_{Si} . Although hourly R_s data from geostationary satellite are becoming available,~~
16 ~~but these are available as sectorial products (i.e. for particular continents) instead of full~~
17 ~~global coverage. Ongoing efforts to develop geostationary based data by merging multiple~~
18 ~~geostationary satellites tend to overcome this limitation.~~

19 Acknowledgements

20 The authors thank HiWET (High resolution modelling and monitoring of water and energy
21 transfers in WETland ecosystems) project funded through the Belgian Science Policy
22 (BELSPO) and FNR under the programme STEREOIII (INTER/STEREOIII/13/03/HiWET)
23 (CONTRACT NR SR/00/301). We thank entire FLUXNET site PIs for sharing the eddy
24 covariance data. This work used eddy covariance data acquired by the FLUXNET community
25 and in particular by the following networks: AmeriFlux (U.S. Department of Energy,
26 Biological and Environmental Research, Terrestrial Carbon Program (DE-FG02-04ER63917
27 and DE-FG02-04ER63911)), AfriFlux, AsiaFlux, CarboAfrica, CarboEuropeIP, CarboItaly,
28 CarboMont, ChinaFlux, Fluxnet-Canada (supported by CFCAS, NSERC, BIOCAP,
29 Environment Canada, and NRCan), GreenGrass, KoFlux, LBA, NECC, OzFlux, TCOS-
30 Siberia, USCCC. We acknowledge the financial support to the eddy covariance data

1 harmonization provided by CarboEuropeIP, FAO-GTOS-TCO, iLEAPS, Max Planck Institute
2 for Biogeochemistry, National Science Foundation, University of Tuscia, Université Laval,
3 Environment Canada and US Department of Energy and the database development and
4 technical support from Berkeley Water Center, Lawrence Berkeley National Laboratory,
5 Microsoft Research eScience, Oak Ridge National Laboratory, University of California–
6 Berkeley and the University of Virginia.

7 KM designed the analysis, LW performed the research, KM and LW developed the
8 manuscript, and all the coauthors jointly contributed in editing the manuscript. The authors
9 declare no conflict of interest.

10

11

1 **References**

2 Ahmad, A., Anderson, T. N., and Lie, T. T.: Hourly global solar irradiation forecasting for
3 New Zealand, *Sol. Ener.*, 122, 1398–1408, doi:10.1016/j.solener.2015.10.055, 2015.

4 Allen, R. G., Pereira, L. S., Raes, D., and Smith, M.: Crop evapotranspiration, Guidelines for
5 computing crop water requirements, FAO Irrigation and drainage paper n. 56. 326 pp.,
6 Rome, Italy, 1998.

7 Anderson, R. G., Lo, M.-H., Swenson, S., Famiglietti, J. S., Tang, Q., Skaggs, T. H., Lin, Y.-
8 H., and Wu, R.-J.: Using satellite-based estimates of evapotranspiration and groundwater
9 changes to determine anthropogenic water fluxes in land surface models, *Geosci. Model
10 Dev.*, 8, 3021-3031, doi:10.5194/gmd-8-3021-2015, 2015.

11 Baigorria, G. A., Villegas, E. B., Trebejo, I., Carlos, J. F., and Quiroz, R.: Atmospheric
12 transmissivity: distribution and empirical estimation around the central Andes, *Int. J.
13 Climatol.*, 24 (9), 1121–1136, doi: <http://doi.org/10.1002/joc.1060>, 2004.

14 Baldocchi, D.D., Falge, E., Gu, L., Olson, R., Hollinger, D., Running, S., et al.: Fluxnet: a
15 new tool to study the temporal and spatial variability of ecosystem-scale carbon dioxide,
16 water vapor, and energy flux densities, *Bull. American Met. Soc.*, 82 (11), 2415–3434,
17 2001.

18 Bisht, G., Venturini, V., Islam, S., and Jiang, L.: Estimation of the net radiation using MODIS
19 (Moderate Resolution Imaging Spectroradiometer) data for clear sky days, *Remote Sens.
20 Environ.*, 97 (1), 52–67, doi:10.1016/j.rse.2005.03.014, 2005.

21 Boulifa, M., Adane, A., Rezagui, A., and Ameur, et. Z.: Estimate of the Global Solar
22 Radiation by Cloudy Sky Using HRV Images, *Ener. Proc.*, 74, 1079–1089,
23 doi:10.1016/j.egypro.2015.07.747, 2015.

24 Brutsaert, W., and Sugita, M.: Application of self-preservation in the diurnal evolution of the
25 surface energy budget to determine daily evaporation, *J. Geophys. Res. Atmos.*, 97
26 (D17), 18377–18382, doi: 10.1029/92JD00255, 1992.

27 Burden, F., and Winkler, D.: Bayesian Regularization of Neural Networks. In D. Livingstone
28 (Ed.), *Artificial Neural Networks SE - 3*, 458, 23–42, Humana Press, doi:10.1007/978-1-
29 60327-101-1_3, 2009.

30 Cammalleri, C., Anderson, M. C., and Kustas, W. P.: Upscaling of evapotranspiration fluxes
31 from instantaneous to daytime scales for thermal remote sensing applications, *Hydrol.
32 Earth Sys. Sci.*, 18 (5), 1885–1894, doi:10.5194/hess-18-1885-2014, 2014.

33 Chávez, J. L., Neale, C. M. U., Prueger, J. H., and Kustas, W. P.: Daily evapotranspiration
34 estimates from extrapolating instantaneous airborne remote sensing ET values, *Irrig.
35 Sci.*, 27 (1), 67–81, doi:10.1007/s00271-008-0122-3, 2008.

36 Chen, Z., Shi, R., and Zhang, S.: An artificial neural network approach to estimate

1 evapotranspiration from remote sensing and AmeriFlux data, *Front. Earth Sci.*, 7 (1),
2 103–111, doi:10.1007/s11707-012-0346-7, 2013.

3 Colaizzi, P. D., Evett, S. R., Howell, T. A., and Tolk, J. A.: Comparison of five models to
4 scale daily evapotranspiration from one-time-of-day measurements, *Trans. ASAE*, 49,
5 1409–1417, doi: 10.13031/2013.22056, 2006.

6 Crago, R. D.: Conservation and variability of the evaporative fraction during the daytime, *J.*
7 *Hydrol.*, 180 (1–4), 173–194, doi:10.1016/0022-1694(95)02903-6, 1996.

8 Dahmani, K., Notton, G., Voyant, C., Dizene, R., Nivet, M. L., Paoli, C., and Tamas, W.:
9 Multilayer Perceptron approach for estimating 5-min and hourly horizontal global
10 irradiation from exogenous meteorological data in locations without solar measurements,
11 *Ren. Ener.*, 90, 267–282. doi:10.1016/j.renene.2016.01.013, 2016.

12 Delogu, E., Boulet, G., Olioso, A., Coudert, B., et al.: Reconstruction of temporal variations
13 of evapotranspiration using instantaneous estimates at the time of satellite overpass,
14 *Hydrol. Earth Syst. Sci.*, 16 (8), 2995–3010, doi:10.5194/hess-16-2995-2012, 2012.

15 Foken, T., Wimmer, F., Mauder, M., Thomas, C., and Liebethal, C.: Some aspects of the
16 energy balance closure problem, *Atm. Chem. Phys.*, 6 (12), 4395–4402,
17 doi:10.5194/acp-6-4395-2006, 2006.

18 Franssen, H. J. H., Stöckli, R., Lehner, I., Rotenberg, E., and Seneviratne, S. I.: Energy
19 balance closure of eddy-covariance data: A multisite analysis for European FLUXNET
20 stations, *Agric. For. Meteorol.*, 150 (12), 1553–1567,
21 doi:10.1016/j.agrformet.2010.08.005, 2010.

22 Gardner, M. W., and Dorling, S. R.: Artificial neural networks (the multilayer perceptron)—a
23 review of applications in the atmospheric sciences, *Atmos. Environ.*, 32 (14–15), 2627–
24 2636, doi:10.1016/S1352-2310(97)00447-0, 1998.

25 Gentine, P., Entekhabi, D., Chehbouni, A., Boulet, G., and Duchemin, B.: Analysis of
26 evaporative fraction diurnal behaviour, *Agric. For. Meteorol.*, 143 (1–2), 13–29,
27 doi:10.1016/j.agrformet.2006.11.002, 2007.

28 Harper, A., Baker, I. T., Denning, A. S., Randall, D. A., Dazlich, D., and Branson, M.: Impact
29 of Evapotranspiration on Dry Season Climate in the Amazon Forest, *J. Clim.*, 27 (2),
30 574–591, doi: 10.1175/JCLI-D-13-00074.1, 2014.

31 Hasni, A., Sehli, A., Draoui, B., Bassou, A., and Amieur, B.: Estimating Global Solar
32 Radiation Using Artificial Neural Network and Climate Data in the South-western
33 Region of Algeria, *Energy Proc.*, 18, 531–537, doi:10.1016/j.egypro.2012.05.064, 2012.

34 Hildebrandt, A., Aufi, M. A., Amerjeed, M., Shammas, M., and Eltahir, E. A. B.:
35 Ecohydrology of a seasonal cloud forest in Dhofar: 1. Field experiment, *Water Resour.*
36 Res., 43, W10411, doi:10.1029/2006WR005261, 2007.

37 Hoedjes, J. C. B., Chehbouni, A., Jacob, F., Ezzahar, J., and Boulet, G.: Deriving daily

1 evapotranspiration from remotely sensed instantaneous evaporative fraction over olive
2 orchard in semi-arid Morocco, J. Hydrol., 354 (1-4), 53-64,
3 doi:10.1016/j.jhydrol.2008.02.016, 2008.

4 Huang, G., Liu, S., and Liang, S.: Estimation of net surface shortwave radiation from MODIS
5 data, Int. J. Remote Sens., 33 (3), 804-825, doi:10.1080/01431161.2011.577834, 2012.

6 Jackson, R. D., Hatfield, J. L., Reginato, R. J., Idso, S. B., and Pinter, P. J. Jr.: Estimation of
7 daily evapotranspiration from one time-of-day measurements, Agric. Wat. Man., 7 (1-3),
8 351-362, doi:10.1016/0378-3774(83)90095-1, 1983.

9 Khatib, T., Mohamed, A., and Sopian, K.: A review of solar energy modeling techniques,
10 Ren. Sust. Energy Rev., 16 (5), 2864-2869, doi: 10.1016/j.rser.2012.01.064, 2012.

11 [Kim, Y., Knox, R. G., Longo, M., Medvigy, D., Hutyra, L. R., Pyle, E. H., Wofsy, S. C.,](#)
12 [Bras, R. L., and Moorcroft, P. R.: Seasonal carbon dynamics and water fluxes in an](#)
13 [Amazon rainforest, Global Change Biol., 18 \(4\), 1322-1334, doi: 10.1111/j.1365-](#)
14 [2486.2011.02629.x, 2012.](#)

15 Laine, V., Venäläinen, A., Heikinheimo, M., and Hyvärinen, O.: Estimation of Surface Solar
16 Global Radiation from NOAA AVHRR Data in High Latitudes, J. Appl. Meteorol., 38
17 (12), 1706-1719, doi: [http://dx.doi.org/10.1175/1520-0450\(1999\)038<1706:EOSSGR>2.0.CO;2](http://dx.doi.org/10.1175/1520-0450(1999)038<1706:EOSSGR>2.0.CO;2), 1999.

19 Lazzús, J. A., Pérez Ponce, A. A., and Marin, J.: Estimation of global solar radiation over the
20 city of La Serena (Chile) using a neural network, Appl. Sol. Ener., 47 (1), 66-73, doi:
21 10.3103/S0003701X11010099, 2011.

22 Li, M.-F., Tang, X.-P., Wu, W., and Liu, H.-B.: General models for estimating daily global
23 solar radiation for different solar radiation zones in mainland China, Energy Conv.
24 Manag., 70, 139-148, doi: 10.1016/j.enconman.2013.03.004, 2013.

25 [Loew, A., Peng, J., and Borsche, M.: High-resolution land surface fluxes from satellite and](#)
26 [reanalysis data \(HOLAPS~v1.0\): evaluation and uncertainty assessment, Geosci. Model](#)
27 [Dev., 9 \(7\), 2499-2532, doi:10.5194/gmd-9-2499-2016, 2016.](#)

28 [Lopez, G., and Batlles, F. J.: Estimating solar radiation from MODIS data, Enrgy Proc., 49,](#)
29 [2362 - 2369, 2014, doi:10.1016/j.egypro.2014.03.250.](#)

30 [Malek, E.: Night-time evapotranspiration vs. daytime and 24h evapotranspiration, J. Hydrol.,](#)
31 [138\(1\), 119-129, doi:10.1016/0022-1694\(92\)90159-S, 1992.](#)

32 [Mallick, K., Jarvis, A., Wohlfahrt, G., Kiely, G., Hirano, T., Miyata, A., Yamamoto, S., and](#)
33 [Hoffmann, L.: Components of near-surface energy balance derived from satellite](#)
34 [soundings – Part 1: Noontime net available energy, Biogeosciences, 12, 433-451,](#)
35 [doi:10.5194/bg-12-433-2015, 2015.](#)

36 Mauder, M., and Foken, T.: Impact of post-field data processing on eddy covariance flux
37 estimates and energy balance closure, Meteorolog. Zeit., 15 (6), 597-609, 2006.

1 McCulloch, W. S., and Pitts, W.: A logical calculus of the ideas immanent in nervous activity,
2 The Bull. Math. Biophys., 5 (4), 115–133, doi: 10.1007/BF02478259, 1943.

3 Mubiru, J., and Banda, E. J. K. B.: Estimation of monthly average daily global solar
4 irradiation using artificial neural networks, Sol. Ener., 82 (2), 181–187, doi:
5 10.1016/j.solener.2007.06.003, 2008.

6 Parlange, M. B., and Katul, G. G.: Estimation of the diurnal variation of potential evaporation
7 from a wet bare soil surface, J. Hydrol., 132 (1-4), 71–89, doi: 10.1016/0022-
8 1694(92)90173-S, 1992.

9 Polo, J., Zarzalejo, L., and Ramírez, L.: Solar Radiation Derived from Satellite Images, In V.
10 Badescu (Ed.), Modeling Solar Radiation at the Earth's Surface SE - 18, 449–462,
11 Springer Berlin Heidelberg, doi: 10.1007/978-3-540-77455-6_18, 2008.

12 Ryu, Y., Baldocchi, D. D., Black, T. A., Detto, M., et al.: On the temporal upscaling of
13 evapotranspiration from instantaneous remote sensing measurements to 8-day mean
14 daily-sums, Agric. For. Meteorol., 152, 212–222, doi: 10.1016/j.agrformet.2011.09.010,
15 2012.

16 Senay, G. B., Velpuri, N. M., Bohms, S., Budde, M., et al.: Drought Monitoring and
17 Assessment: Remote Sensing and Modeling Approaches for the Famine Early Warning
18 Systems Network, In: Hydro-Meteorological Hazards, Risks, and Disasters, 233 - 262,
19 doi: 10.1016/B978-0-12-394846-5.00009-6, 2015.

20 Sepulcre-Canto, G., Vogt, J., Arboleda, A., and Antofie, T.: Assessment of the EUMETSAT
21 LSA-SAF evapotranspiration product for drought monitoring in Europe, Int. J. Appl.
22 Earth Obs. Geoinf., 30, 190–202, doi: 10.1016/j.jag.2014.01.021, 2014.

23 Shamshirband, S., Mohammadi, K., Tong, C. W., Zamani, M., et al.: A hybrid SVM-FFA
24 method for prediction of monthly mean global solar radiation, Theor. Appl. Climatol., 1–
25 13, doi: 10.1007/s00704-015-1482-2, 2015.

26 Shuttleworth, W. J., Gurney, R. J., Hsu, A. Y., and Ormsby, J. P.: FIFE: the variation in
27 energy partition at surface flux sites, IAHS Publ., 186, 67–74, 1989.

28 Tang, R., Li, Z.-L., and Sun, X.: Temporal upscaling of instantaneous evapotranspiration: An
29 intercomparison of four methods using eddy covariance measurements and MODIS data,
30 Remote Sens. Environ., 138, 102–118, doi: 10.1016/j.rse.2013.07.001, 2013.

31 Tang, R., Tang, B., Wu, H., Li, Z. L.: On the feasibility of temporally upscaling instantaneous
32 evapotranspiration using weather forecast information, Int. J. Remote Sens., 36 (19-20),
33 doi: 10.1080/01431161.2015.1029597, 2015.

34 Tolk, J. A., Howell, T. A., and Evett, S. R.: Nighttime evapotranspiration from alfalfa and
35 cotton in a semiarid climate, Agron. J., 98(3), 730 - 736, doi:10.2134/agronj2005.0276
36 2006.

37 Van Niel, T. G., McVicar, T. R., Roderick, M. L., van Dijk, A. I. J. M., et al.: Upscaling latent

1 heat flux for thermal remote sensing studies: Comparison of alternative approaches and
2 correction of bias, *J. Hydrol.*, 468–469, 35–46, doi: 10.1016/j.jhydrol.2012.08.005, 2012.

3 Wang, S.-C.: Artificial Neural Network. In: *Interdisciplinary Computing in Java*
4 Programming SE - 5, 743, 81–100, Springer US, doi: 10.1007/978-1-4615-0377-4_5,
5 2003.

6 [Wang, D., Liang, S., He, T., Cao, Y., and Jiang, B.: Surface Shortwave Net Radiation](#)
7 [Estimation from FengYun-3 MERSI Data, Remote Sens., 7, 6224-6239,](#)
8 [doi:10.3390/rs70506224, 2015](#)

9 Wilson, K., Goldstein, A., Falge, E., Aubinet, M., et al.: Energy balance closure at FLUXNET
10 sites, *Agric. For. Meteorol.*, 113 (1–4), 223–243, doi: 10.1016/S0168-1923(02)00109-0,
11 2002.

12 Xu, T., Liu, S., Xu, L., Chen, Y., Jia, Z., Xu, Z., & Nielson, J.: Temporal Upscaling and
13 Reconstruction of Thermal Remotely Sensed Instantaneous Evapotranspiration, *Remote*
14 *Sens.*, 7 (3), 3400, doi: 10.3390/rs70303400, 2015.

15

16

17

18

19

20

21

22

23

24

25

26

27

28

29

30

31

32

33

34

35

36

37

38

39

40

1 **Table 1:** Statistical analysis of the performance of ANN in predicting R_{Sd} under varying sky
 2 conditions represented by four different classes of daily atmospheric transmissivity (τ). Here the
 3 statistical metrics of R_{Sd_pred} for two different upscaling hours (1100 and 1330 h) are presented.

<u>Time-of-daytime</u> <u>Time-of-day</u> (h)	τ	R^2	RMSE ($MJ\ m^{-2}\ d^{-1}$)	IA	MAPE	Bias ($MJ\ m^{-2}\ d^{-1}$)
1100	τ_1	0.67	1.84	0.67	53.56	1.12
	τ_2	0.79	2.45	0.80	16.69	0.59
	τ_3	0.88	2.30	0.82	9.17	-0.74
	τ_4	0.98	0.63	0.95	1.69	0.08
1330	τ_1	0.65	1.77	0.67	51.50	1.06
	τ_2	0.81	2.44	0.81	16.83	0.69
	τ_3	0.89	2.23	0.83	8.94	-0.85
	τ_4	0.98	0.89	0.95	2.40	-0.46

4
 5
 6
 7
 8
 9
 10
 11
 12

1 | **Table 2:** A summary of ET_d error statistics by comparing the performance of R_S -based, R_S TOA-based and EF -based ET_d
 2 upscaling methods with regard to different sky conditions. Here τ_1 represents low atmospheric transmissivity due to high
 3 cloudiness while τ_4 represents high transmissivity under clear sky conditions.

Time-of-daytime Time-of-day (h)	τ	R ²			RMSE (MJ m ⁻² d ⁻¹)			IA			MAPE			Bias (MJ m ⁻² d ⁻¹)		
		R_S	R_S TOA	EF	R_S	R_S TOA	EF	R_S	R_S TOA	EF	R_S	R_S TOA	EF	R_S	R_S TOA	EF
1100	τ_1	0.49	0.32	0.32	1.34	1.65	2.07	0.72	0.67	0.71	50.14	66.70	64.19	-0.13	-0.04	0.05
	τ_2	0.72	0.70	0.69	1.73	1.81	1.93	0.81	0.78	0.69	26.47	32.41	36.42	-0.21	-0.19	-0.95
	τ_3	0.72	0.73	0.79	1.99	1.94	2.38	0.81	0.79	0.59	24.69	25.66	40.37	-0.24	-0.37	-1.78
	τ_4	0.77	0.81	0.68	1.32	1.13	2.00	0.84	0.81	0.49	32.17	30.02	55.43	0.05	-0.19	-1.34
1330	τ_1	0.52	0.34	0.29	1.21	1.68	2.34	0.73	0.69	0.71	48.29	66.09	68.14	-0.11	0.08	0.12
	τ_2	0.73	0.72	0.71	1.71	1.93	1.86	0.82	0.79	0.71	26.12	33.71	35.33	-0.01	0.24	-0.88
	τ_3	0.75	0.75	0.76	1.89	1.96	2.43	0.82	0.82	0.61	23.17	25.82	41.65	0.09	0.14	-1.75
	τ_4	0.79	0.86	0.80	1.32	1.09	1.86	0.84	0.86	0.49	29.54	26.59	53.91	0.10	0.11	-1.38

4
 5
 6
 7
 8
 9
 10
 11
 12

1 **Table 3:** Error statistics of $ET_{d,pred}$ at four different temporal scales from three ET_i upscaling methods.

$\frac{\text{Time-of-daytime}}{\text{Time-of-day}}$ (h)	Temporal scale	R ²			RMSE (MJ m ⁻² d ⁻¹)			IA			MAPE			Bias (MJ m ⁻² d ⁻¹)		
		R_S	$R_{S\text{TOA}}$	EF	R_S	$R_{S\text{TOA}}$	EF	R_S	$R_{S\text{TOA}}$	EF	R_S	$R_{S\text{TOA}}$	EF	R_S	$R_{S\text{TOA}}$	EF
1100	Daily	0.71	0.72	0.71	1.79	1.85	2.16	0.82	0.80	0.67	28.80	32.98	57.00	0.19	0.22	1.21
	8-days	0.86	0.84	0.85	1.17	1.22	1.65	0.87	0.86	0.67	18.50	20.63	46.96	0.19	0.22	1.16
	Monthly	0.89	0.88	0.88	0.99	1.04	1.61	0.89	0.67	0.67	15.52	17.22	49.72	0.19	0.22	1.16
	Annually	0.92	0.91	0.93	0.57	0.62	1.33	0.87	0.84	0.54	11.12	12.54	45.88	0.19	0.22	1.21
1330	Daily	0.75	0.74	0.69	1.74	1.89	2.2	0.83	0.82	0.67	26.59	29.89	56.45	-0.04	0.17	-1.18
	8-days	0.87	0.86	0.84	1.11	1.21	1.7	0.88	0.88	0.68	16.80	17.97	50.36	-0.04	0.17	-1.18
	Monthly	0.90	0.90	0.87	0.93	1.00	1.59	0.90	0.89	0.68	13.69	14.85	48.08	-0.04	0.17	-1.18
	Annually	0.93	0.93	0.92	0.51	0.53	1.31	0.88	0.88	0.54	9.00	9.70	44.13	-0.04	0.17	-1.18

2

3

4

5

6

7

8

9

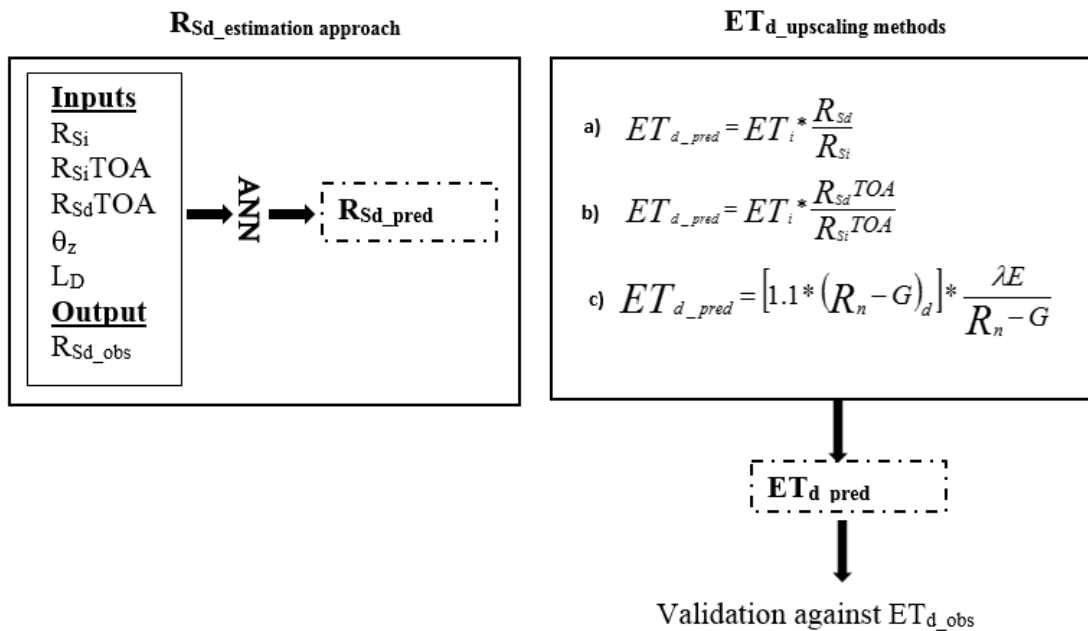
1 **Table 4:** Evaluation of the R_s -based ANN predicted ET_d ($ET_{d,pred}$) error statistics based on ‘closed’ (EBC) and unclosed’ (EBO) surface energy balance
 2 under varying sky conditions represented by four different classes of daily atmospheric transmissivity (τ). Here τ_1 represents low atmospheric
 3 transmissivity due to high cloudiness while τ_4 represents high transmissivity under clear sky conditions. The statistical metrics of $ET_{d,pred}$ for two
 4 different upscaling hours (1100 and 1330 h) are presented.

Time-of-day (h)	τ	R^2		RMSE (MJ m ⁻² d ⁻¹)		IA		MAPE		Bias (MJ m ⁻² d ⁻¹)	
		EBO	EBC	EBO	EBC	EBO	EBC	EBO	EBC	EBO	EBC
1100	τ_1	0.37	0.17	2.96	3.31	0.71	0.57	87.21	86.49	0.66	1.12
	τ_2	0.68	0.54	1.64	2.94	0.78	0.68	28.66	38.01	-0.10	0.65
	τ_3	0.75	0.61	1.77	3.20	0.76	0.66	25.31	37.82	-0.67	1.34
	τ_4	0.66	0.61	1.09	3.40	0.71	0.30	21.77	85.80	-0.31	3.83
1330	τ_1	0.35	0.25	2.02	2.70	0.71	0.60	69.78	78.18	0.37	0.87
	τ_2	0.76	0.5	1.54	3.27	0.81	0.69	27.56	40.98	0.23	0.63
	τ_3	0.77	0.59	1.66	3.18	0.80	0.70	23.16	34.17	-0.46	0.76
	τ_4	0.84	0.64	0.98	2.46	0.76	0.66	23.30	43.89	-0.56	1.23

5
 6

1

Figure 1. A conceptual diagram of the methodology. On the left side is a representation of predicting daily incoming short wave radiation (R_{Sd_pred}). The ANN is trained to learn the system response to a combination of explanatory variables i.e. instantaneous incoming short wave radiation (R_{Si}), instantaneous exo-atmospheric shortwave radiation (R_{SiTOA}), daily exo-atmospheric shortwave radiation (R_{SdTOA}), solar zenith angle (θ_z), and day length (L_D), by being fed with a sample data of observed daily incoming short wave radiation (R_{Sd_obs}) which is the dependant variable. On the right side are methods of upscaling instantaneous (ET_i) to daily ET (ET_d) using our R_S -based method (a) and other two approaches (b, c) are the R_{STOA} and EF -based methods respectively used which are used for comparison.



2

3

4

5

6

7

8

9

10

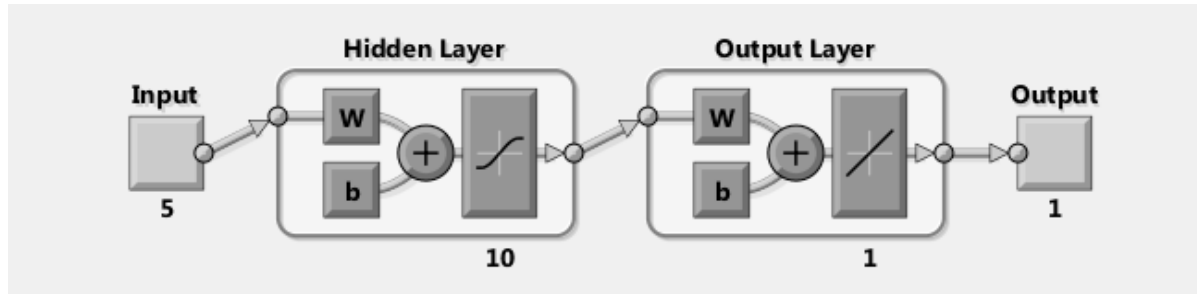
11

12

13

1

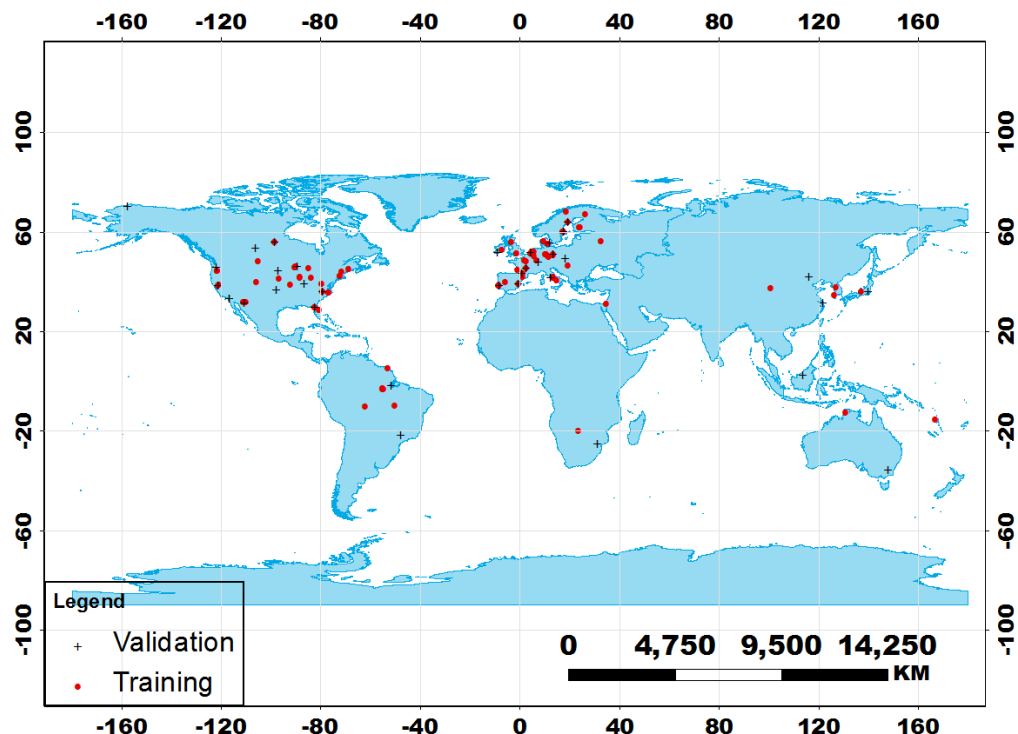
Figure 2. Schematic representation of a simple artificial network model. The artificial neuron has five input variables, for the intended output. These inputs are then assigned weights (W) and bias (b), and the sum of all these products (\sum) is fed to an activation function (f). The activation function alters the signal accordingly and passes the signal to the next neuron(s) until the output of the model is reached (Mathworks, 2015).



2

1

Figure 3. Distribution of 126 sites of the FLUXNET eddy covariance network used in the present study with 85 and 41 sites for training and validation, respectively between the years 1999 and 2006.



2

3

4

5

6

7

8

9

10

11

12

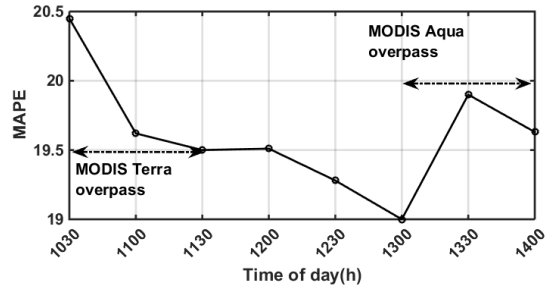
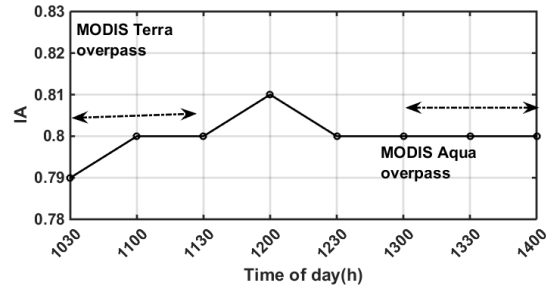
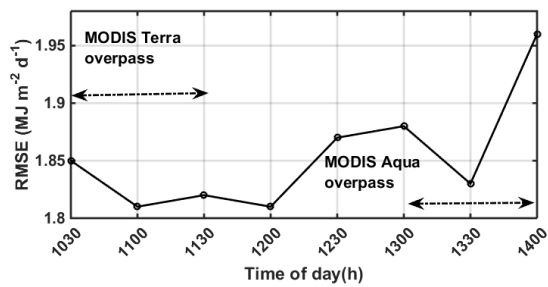
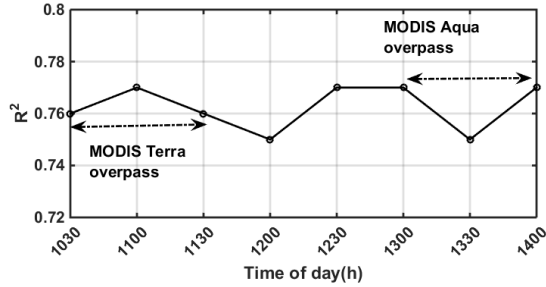
13

14

15

1

Figure 4. Statistical metric of R_{Sd_pred} by ANN for different ~~time-of-day~~ time-of-day. As the study is intended for remote sensing application, we demonstrate the potential of the method for future research in the case where satellite will be used and as such we pick MODIS overpass time as an example to highlight on the predictive ability of the ANN at the specific overpass times.



2

3

4

5

6

7

8

9

10

11

12

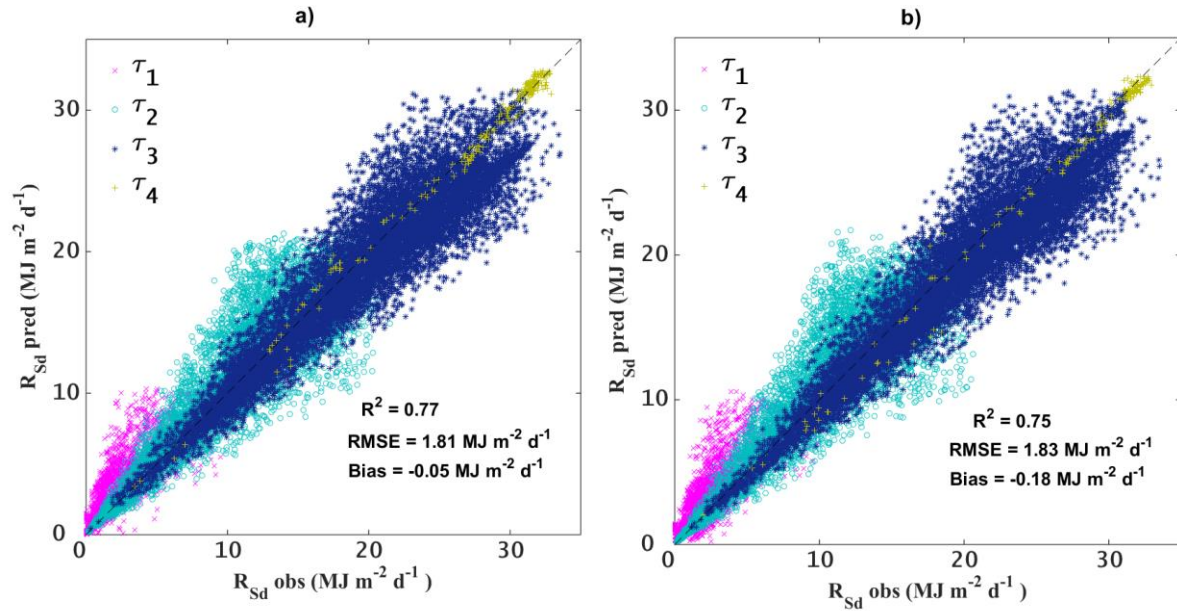
13

14

15

1

Figure 5. Scatter plots between R_{Sd_obs} versus R_{Sd_pred} versus R_{Sd_obs} for different levels of daily atmospheric transmissivity classes (τ) from (a) 1100 and (b) 1330 hours upscaling. Here τ_1 – τ_4 represent daily atmospheric transmissivity of four different class, $0.25 \geq \tau \geq 0$, $0.50 \geq \tau \geq 0.25$, $0.75 \geq \tau \geq 0.50$, and $1 \geq \tau \geq 0.75$, respectively, with τ_1 signifying high degree of cloudiness (or overcast skies) whereas τ_4 indicates clear skies.



2

3

4

5

6

7

8

9

10

11

12

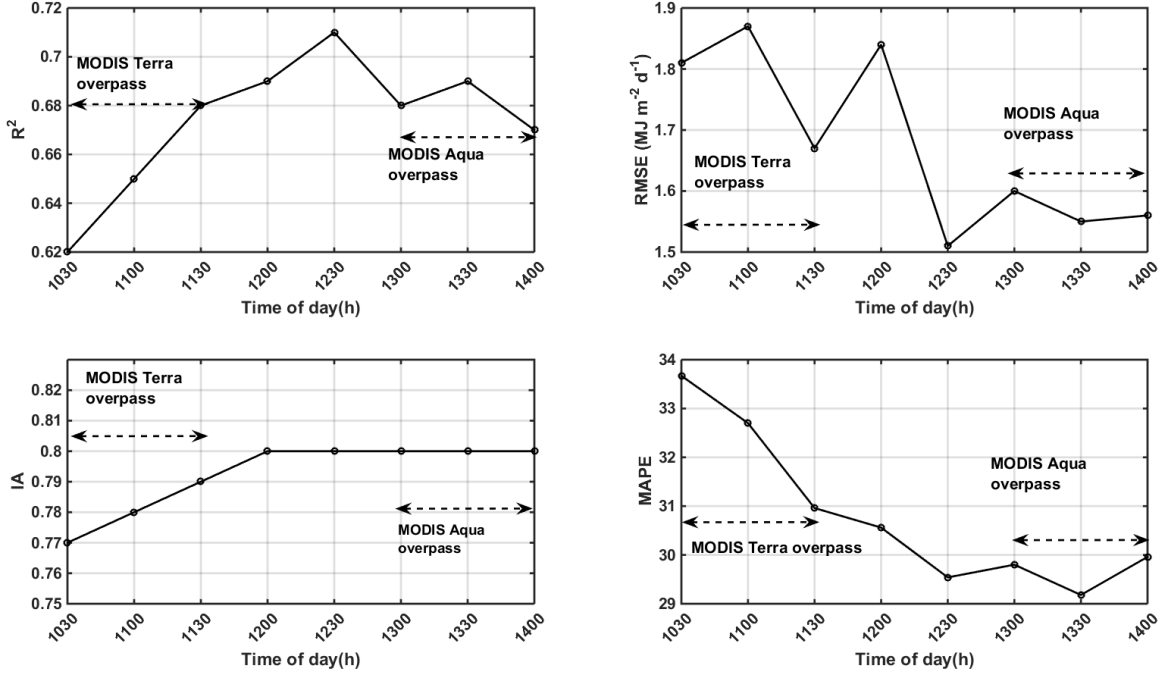
13

14

15

1

Figure 6. Statistical summary of $ET_{d,pred}$ for different ~~time of day~~^{time} using Eq. (1) based on R_{Si} and $R_{Sd,pred}$. As the study is intended for remote sensing application, we once again demonstrate the potential of the method for future research in the case where satellite will be used and as such we pick MODIS Terra-Aqua overpass time.



2

3

4

5

6

7

8

9

10

11

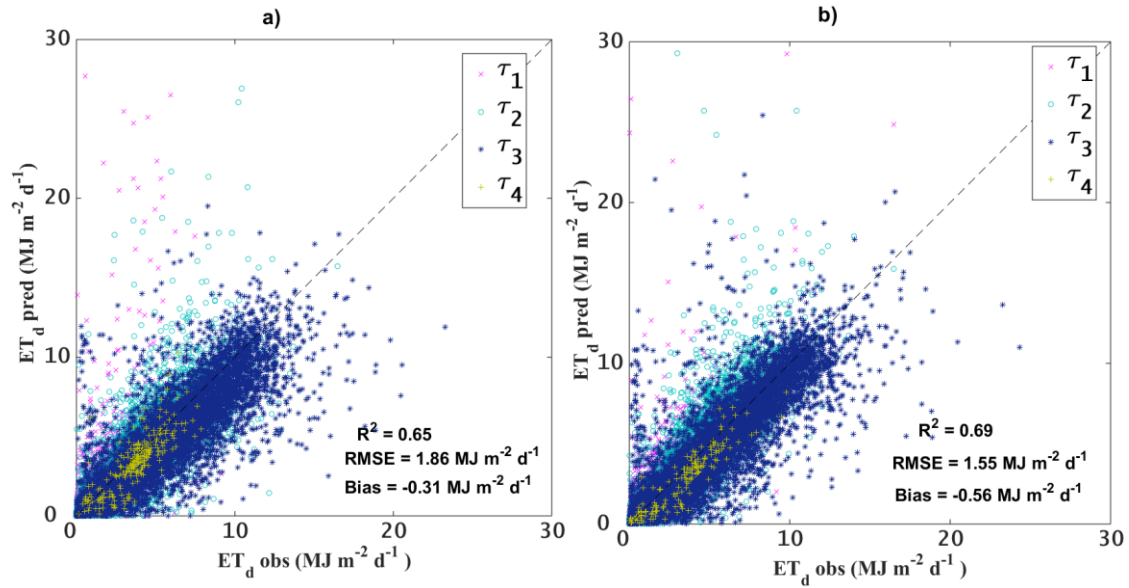
12

13

14

1

Figure 7. ET_{d_pred} obtained through eq. (1) versus ET_{d_obs} for different levels of τ from both forenoon (a) and afternoon (b) upscaling (1100 and 1300 h daytime hours).



2

3

4

5

6

7

8

9

10

11

12

13

14

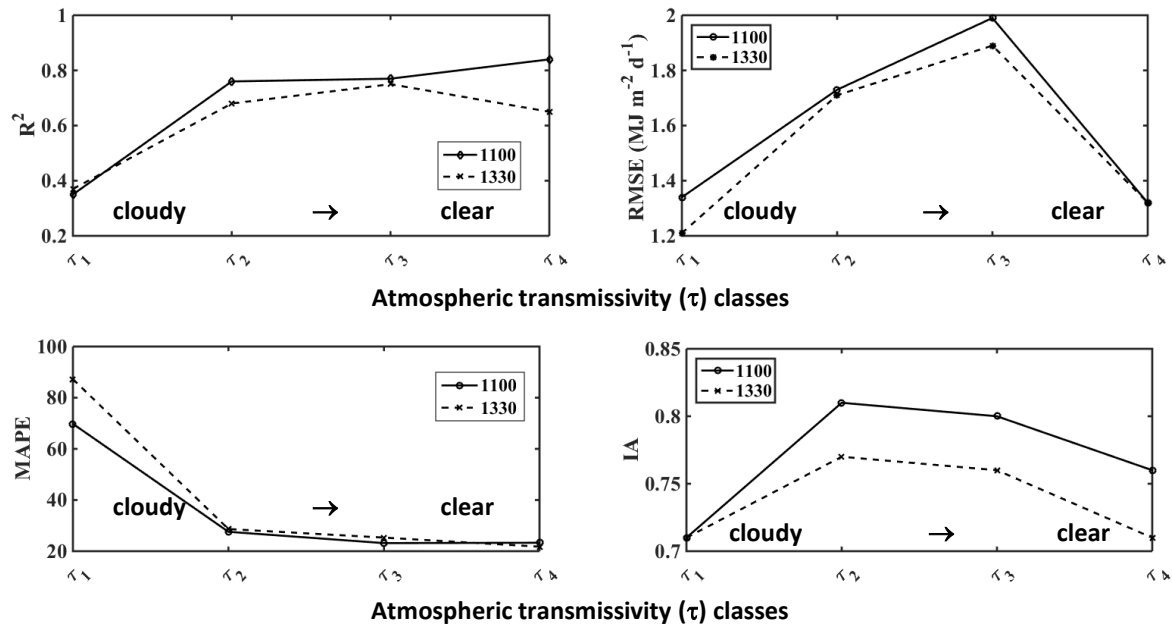
15

16

17

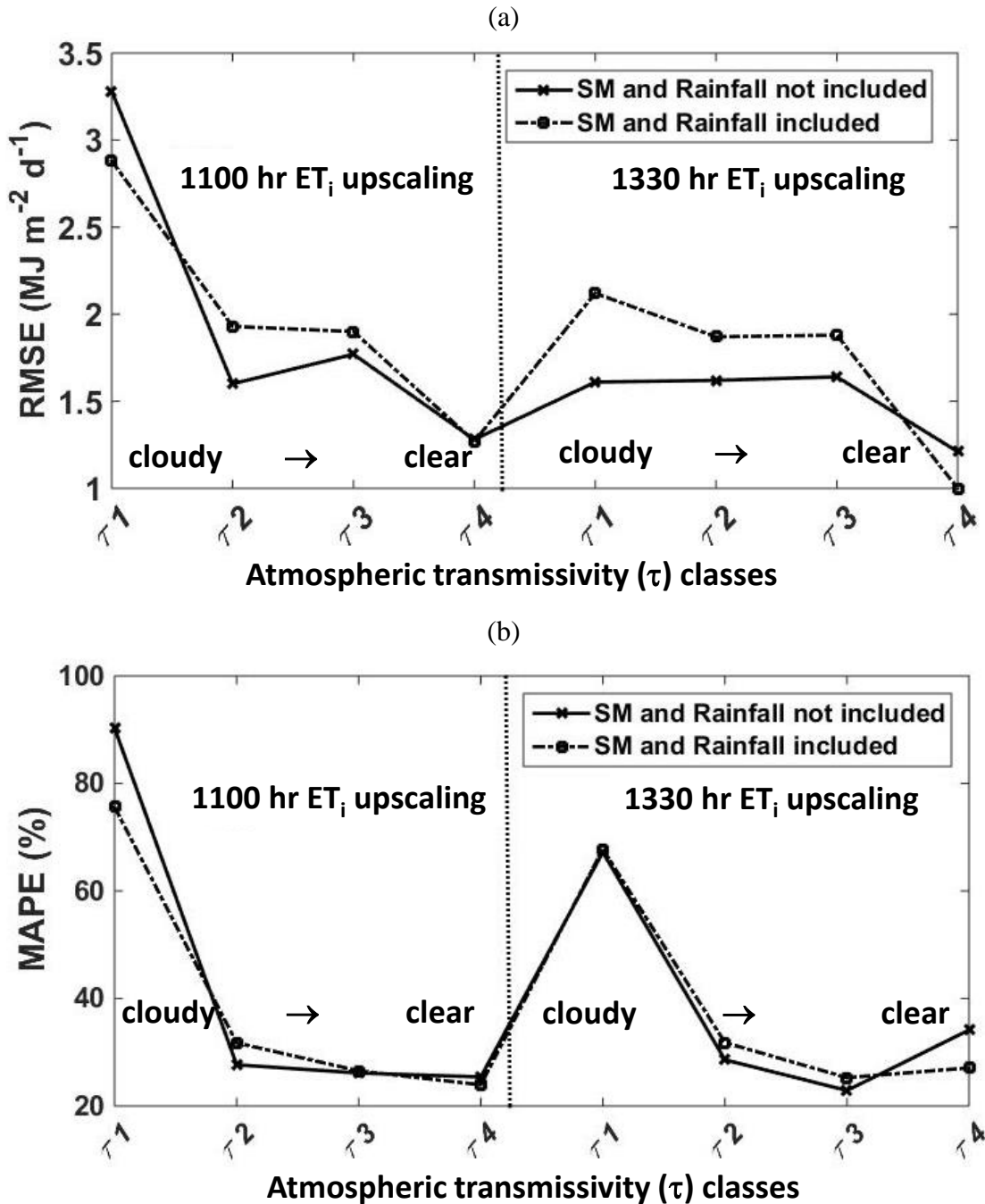
1

Figure 8. Assessing the statistical metrics of ET_{d_pred} (using eq.1) for different levels of daily atmospheric transmissivity classes (representing cloudy to clear skies) for both 1100h and 1330h ~~time-of-day~~ ET_i scaling.



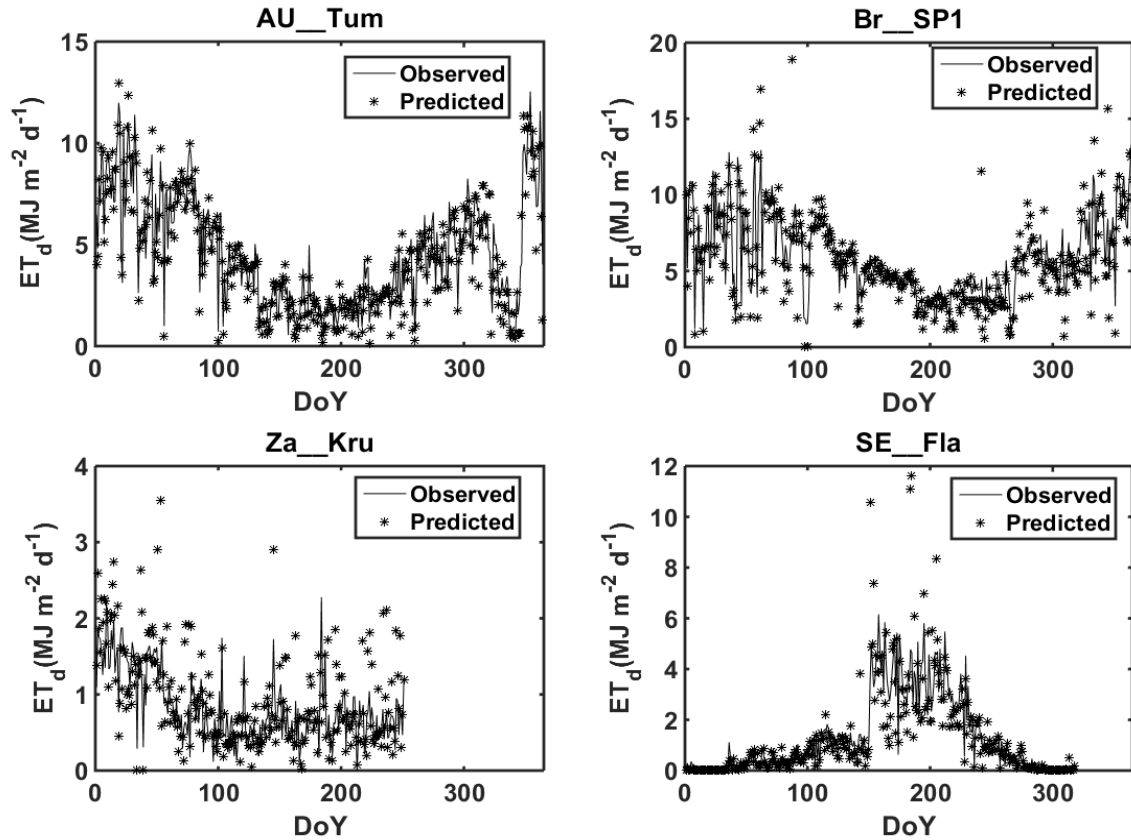
2
3
4
5
6
7
8
9
10
11
12
13
14
15
16

Figure 9. An intercomparison of ET_{d_pred} error statistics (RMSE and MAPE) for different levels of atmospheric transmissivity classes based on two different ANN training (ANN trained with shortwave radiation and astronomical variables only; and ANN trained with radiation, astronomical variables, soil moisture and rainfall) based on 1100h and 1330h time-of-day ET_i scaling.



1

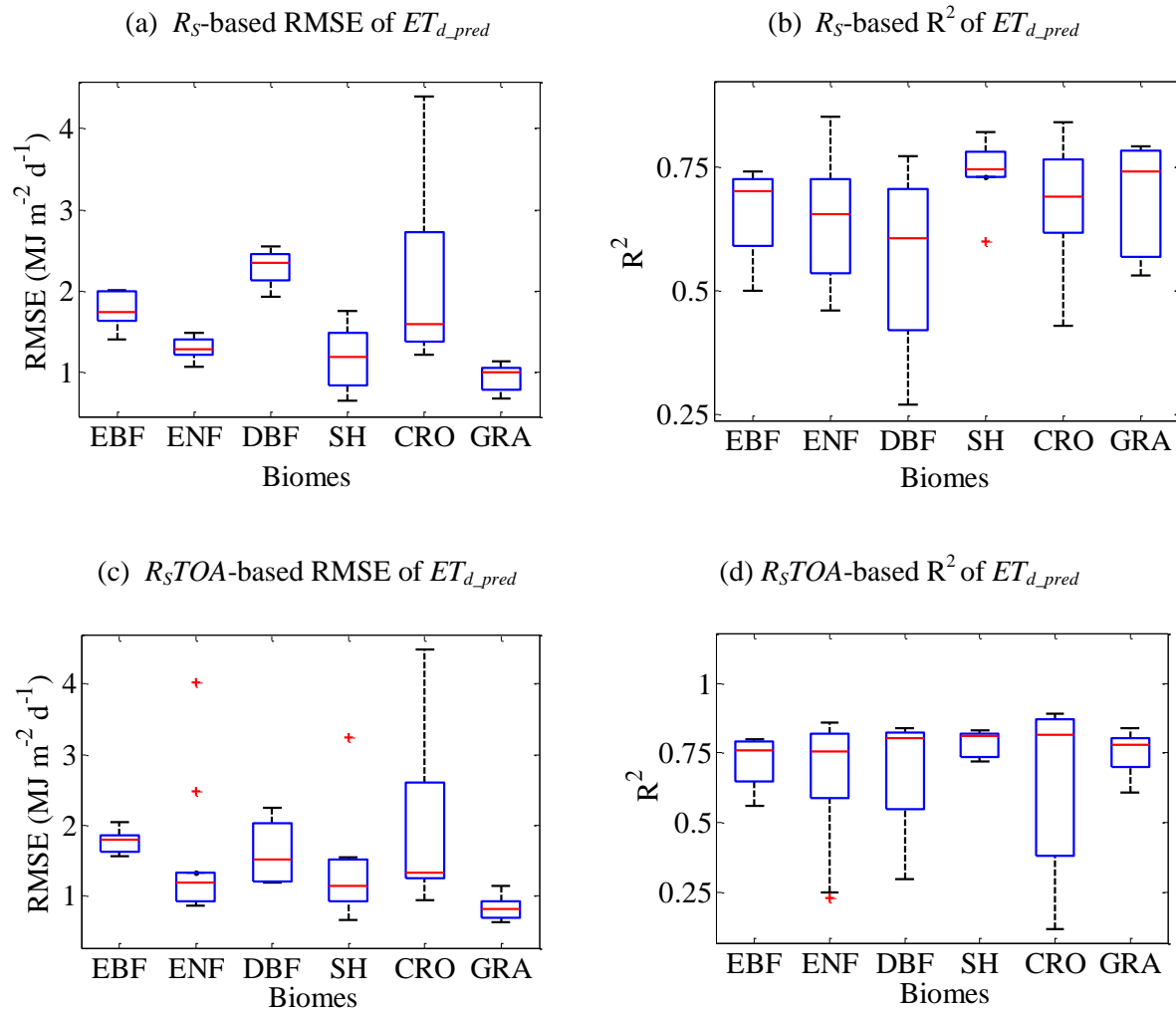
Figure 10. Time series comparison between observed and predicted ET_d for four representative sites located in Australia, Brazil, South Africa and Sweden.



2
3
4
5
6
7
8
9
10
11
12
13
14
15
16
17
18
19

1

Figure 11. Biome specific error characteristics of ET_{d_pred} displaying the box plots of RMSE and coefficient of determination (R^2) from both R_S -based and R_{STOA} -based ET_i upscaling. The biome classes are evergreen broadleaf forest (EBF), evergreen needleleaf forest (ENF), deciduous broadleaf forest (DBF), shrubland (SH), cropland (CRO), and grassland (GRA), respectively.



2
3
4
5
6
7
8
9
10
11
12

Figure 12. Statistical metrics of $ET_{d,pred}$ from three different ET_i upscaling approaches [shortwave incoming radiation (R_s), exo-atmospheric shortwave radiation (R_s TOA) and evaporative fraction (EF)] at different temporal scales based on ET_i measurements at (a) 1100h and (b) 1330h ~~time-of-day~~ ~~time-of-day~~.

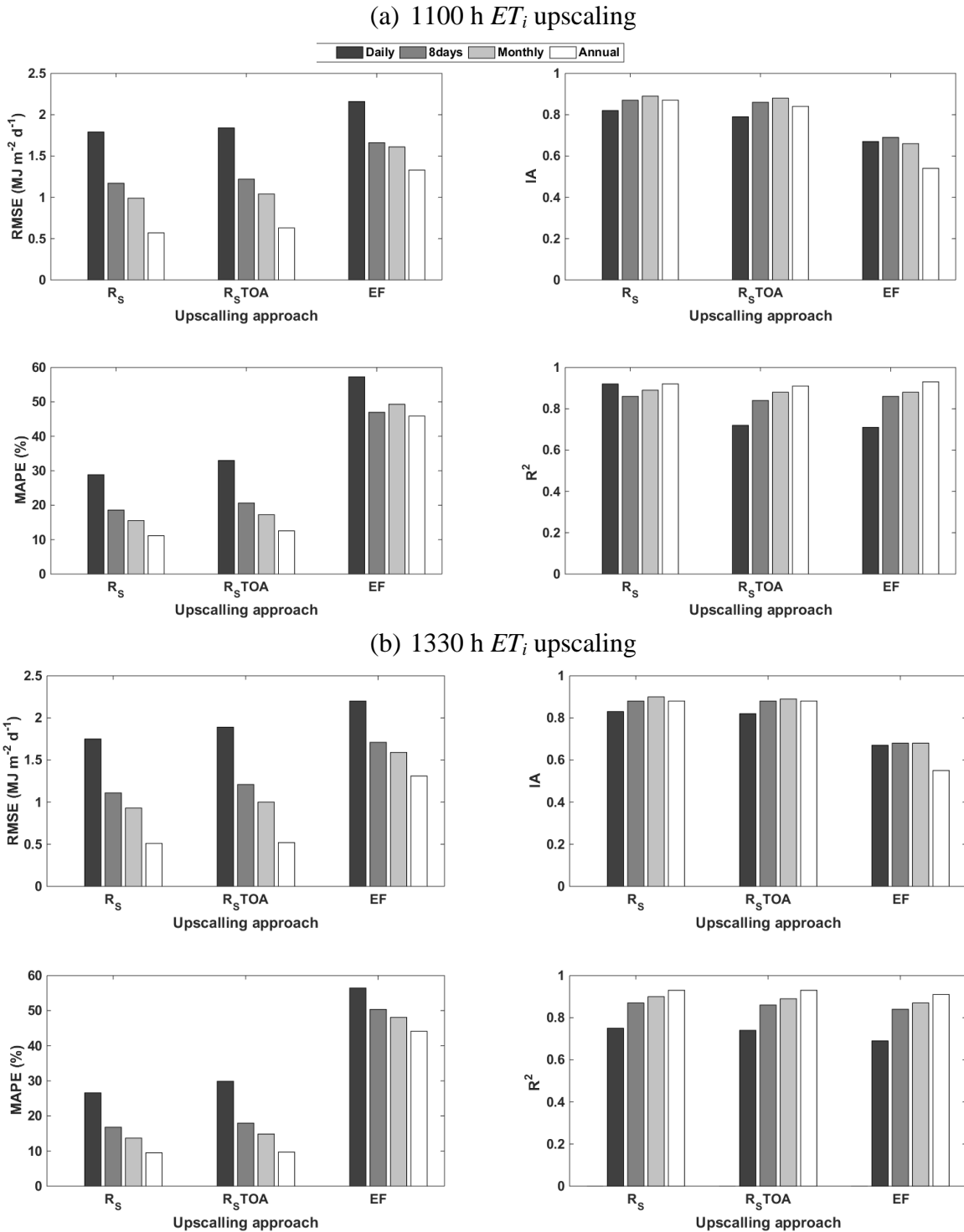
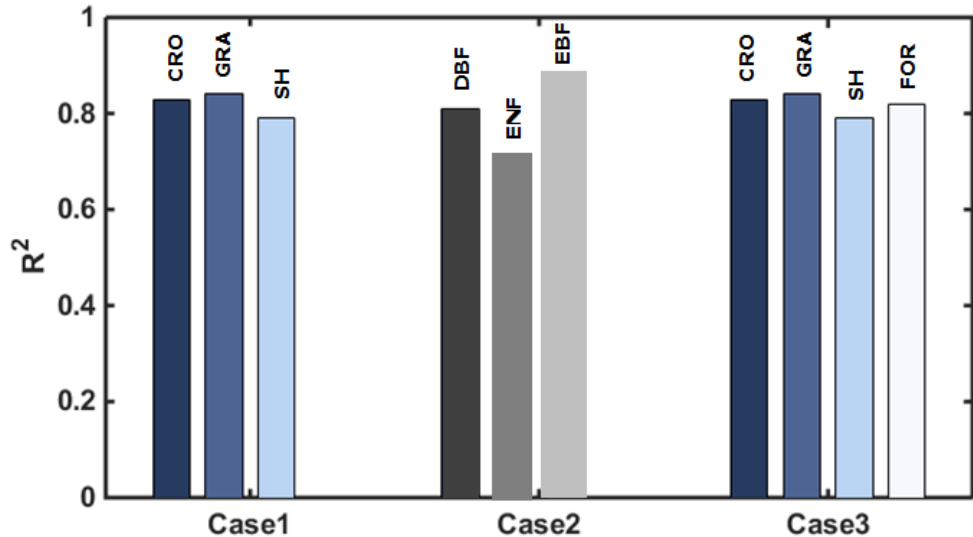


Figure 13. Illustrative examples of the sensitivity of $ET_{d,pred}$ error statistics (R^2 and RMSE) to the different biome type scenarios of ANN training. Here, Case1 consist of training the ANN with forest (FOR) datasets and evaluating ANN predicted ET_d statistics on non-forest biomes, Case2 consist of training the ANN with non-forest datasets and evaluating ANN predicted ET_d statistics on forest biomes, Case3 consist of training the ANN with both forests and non-forest datasets and evaluating ANN predicted ET_d statistics on all the biomes.

(a) R^2 of $ET_{d,pred}$ for three different ANN training scenarios



(b) RMSE of $ET_{d,pred}$ for three different ANN training scenarios

